Chapter 9

Models of Vergence and Accommodation-Vergence Interactions

Bai-chuan Jiang[1], George K. Hung[2], Kenneth J. Ciuffreda[3]

[1]*College of Optometry, Health Professions Division, Nova Southeastern University, 3200 South University Dr., Ft. Lauderdale, FL 33328, PH: (954) 262-1444, FX: (954) 262-1818, EM: bjiang@nova.edu*

[2]*Department of Biomedical Engineering, Rutgers University, 617 Bowser Rd. Piscataway, NJ 08854, PH: (732) 445-4137, FX: (732) 445-3753, EM: shoane@rci.rutgers.edu*

[3] *Dept. of Vision Sciences, State University of New York, State College of Optometry, 33 West 42nd St. New York, NY 10036; PH: (212) 780-5132, FX: (212) 780-5124; EM: kciuffreda@sunyopt.edu*

9.1 INTRODUCTION

Vergence (or disjunctive) eye movements provide single vision by bringing the images of a bifixation target onto corresponding retinal points in the two eyes. When a target moves in depth, the brain recognizes the change in position of the retinal images and drives the extraocular muscles to bring these images into proper register on the retinas. Since vergence eye movements reflect the function of the brain, quantitative assessment of these movements can reveal fundamental information regarding the brain's underlying neural control strategy. For this reason, an understanding of how vergence is controlled in both normal and symptomatic individuals has been one of the most important goals of vision scientists, clinicians, and bioengineers. This chapter provides a summary of some of the most significant research on modeling of the vergence system, as well as the interactions between accommodation and vergence.

9.1.1 Components of Vergence

According to Maddox (1893), the overall or aggregate vergence eye movement is composed of four linearly additive and sequential components: tonic, accommodative, reflex, and voluntary. Tonic vergence is the initial component of vergence which shifts the eyes from an unknown anatomic resting position to a more convergent physiological position of rest; it probably reflects baseline midbrain neural activity. Accommodative vergence is the blur-driven component, which is then added to the tonic vergence component. Maddox recognized that accommodative vergence was due to the amount of accommodation in force during near vision. He was not aware, however, that vergence affected accommodation as well, and hence did not consider interactive feedback effects. Reflex vergence responds to the presence of retinal disparity, or the angular difference between target angle and bifixation angle, and is considered "supplemental" to the other two components. It is now commonly referred to as fusional vergence by clinicians who emphasize its function (Hofstetter, 1945), and disparity vergence by bioengineers who emphasize its stimulus control properties (Stark et al, 1980), which reduces the residual amount of vergence error to a minimum (see Fig. 9.1). The fourth component, voluntary convergence, is attributed to "knowledge of nearness" of the target. It is also referred to as psychic or proximal vergence. Maddox "apparently had as

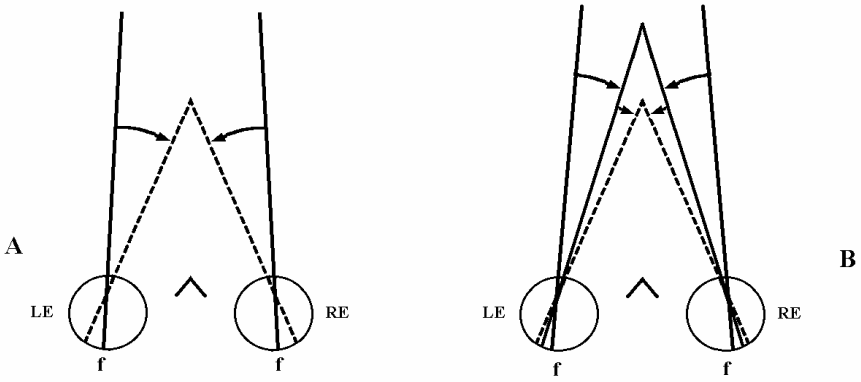

Figure 9.1. (a) Pure symmetrical vergence response showing a complete movement from a far fixation position to a near fixation position. (b) The same pure symmetric response showing sequential components based on the Maddox hierarchy: starting from the tonic vergence position (outer pair of solid lines), it proceeds with an initial accommodative vergence component movement (inner pair of solid lines), which is then followed by the reflex component (now commonly referred to as fusional or disparity convergence) movement (pair of dashed lines) to finally bifixate on the near target. The voluntary vergence component is not shown. The symbol f = fovea.

much difficulty placing psychic or proximal vergence as modern investigators" (Morgan, 1983). Maddox emphasized accommodative convergence and underestimated the role of disparity vergence in the overall vergence movement. However, Maddox's classification remains a useful technique for the analysis of binocular vision problems often encountered in optometric clinics (Morgan, 1983), as well as for the understanding of the interaction between accommodative vergence and the compensatory fusional vergence movement. It has also provided an elementary step in the modeling of the vergence system.

9.1.2 Vergence Dynamics

Vergence dynamics exhibit specific characteristics for each type of stimulus. The pulse response reflects the stimulus duration and amplitude (Fig. 9.2; Rashbass and Westheimer, 1961). That is, a longer duration pulse stimulus elicits a longer response; and a higher amplitude pulse results in a larger response. Step responses have a reaction time ranging from 160 to 200 msec for convergence and from 180 to 210 msec for divergence (Rashbass and Westheimer, 1961; Zuber and Stark, 1968) (Fig. 9.3 and Fig. 9.4 top trace). They exhibit relatively slow and smooth dynamics, having a time constant of about 200 msec for convergence and 240 msec for divergence (Semmlow and Wetzel, 1979). Moreover, for ramp stimulus velocities greater than about 2.7 deg/sec (Semmlow et al, 1986), vergence responses show multiple step movements even though the stimulus is a smooth ramp (Fig. 9.4; Rashbass and Westheimer, 1961).

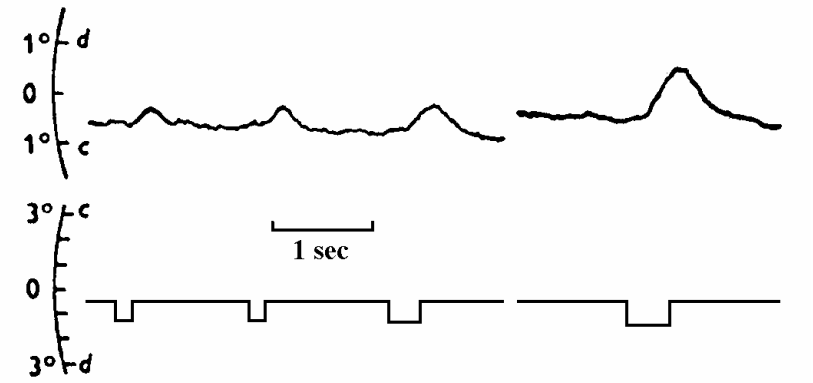

Figure 9.2. Eye movement responses (top trace) to disparity pulse stimuli (bottom trace) of various durations. Reprinted from Rashbass and Westheimer (1961), pg. 345, Fig. 7, with permission of The Physiological Society.

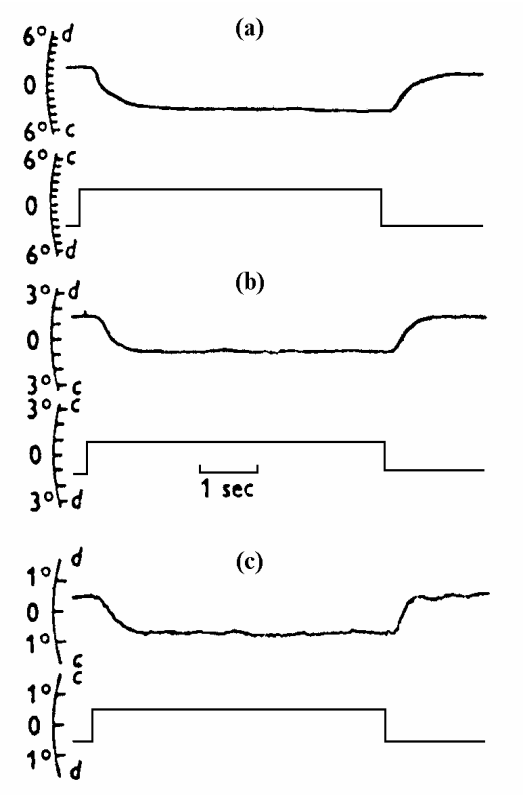

Figure 9.3. Eye movement responses (top traces) to disparity step stimuli (bottom traces) of amplitudes: (a) 4 deg., (b) 2 deg., and (c) 1 deg. Symbol "c" denotes convergence and "d" denotes divergence. Note changes in vertical scale. Reprinted from Rashbass and Westheimer (1961), pg. 344, Fig. 5a, with permission of The Physiological Society.

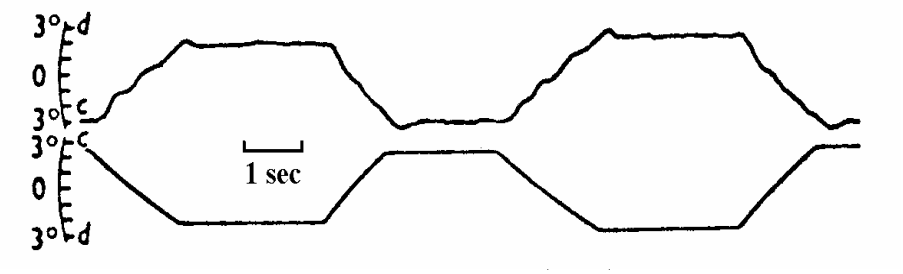

Figure 9.4. Eye movement responses (top trace) to divergent (d) and convergent (c) ramp disparity stimuli (bottom trace). Note the staircase-like multiple-step responses to the ramp stimulus. Reprinted from Rashbass and Westheimer (1961), pg. 346, Fig. 9, with permission of The Physiological Society.

Finally, sinusoidal responses show smooth tracking for the lower frequency sinusoids, but multiple step-like responses to the higher frequency sinusoids (Fig. 9.5).

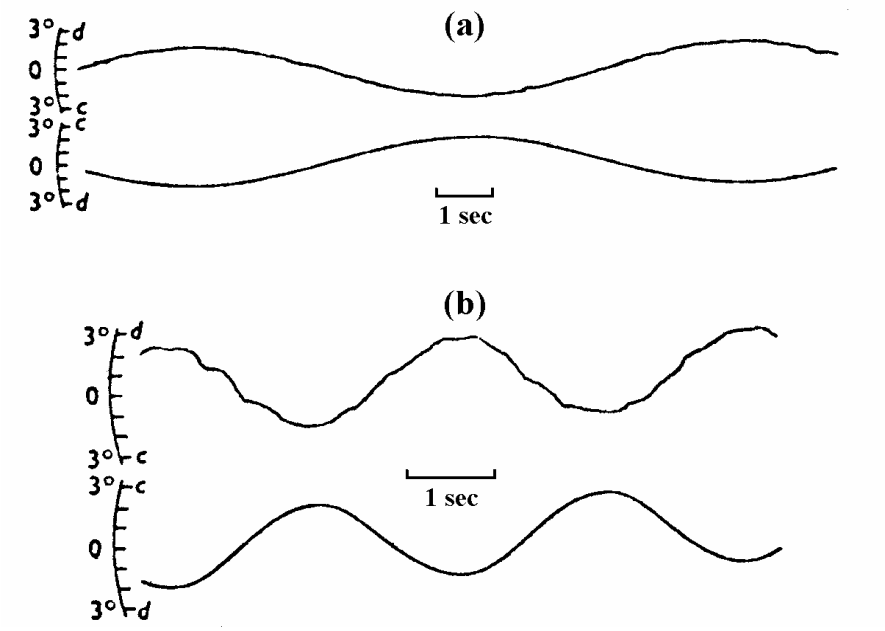

Figure 9.5. Eye movement responses (top traces) to disparity sinusoidal stimuli (bottom traces) at two different amplitudes and frequencies (a and b). Symbol "c" denotes convergence and "d" denotes divergence. Reprinted from Rashbass and Westheimer (1961), pg.. 346, Fig. 10, with permission of The Physiological Society.

The above records were obtained under normal closed-loop conditions. To investigate the control mechanism further, Rashbass and Westheimer (1961) used instrument feedback to maintain a constant vergence error while recording the response. Their results showed a proportionality between the amplitude of the clamped disparity and the velocity of the induced vergence response (Fig. 9.6). To account for these open-loop results, they proposed in their model an integrator in the forward loop of the vergence system. This was because integration of a step of clamped disparity would result in a ramp, or constant velocity, output. Moreover, increasing the clamped disparity step amplitude would increase proportionally the velocity of the response, as seen in Fig. 9.6.

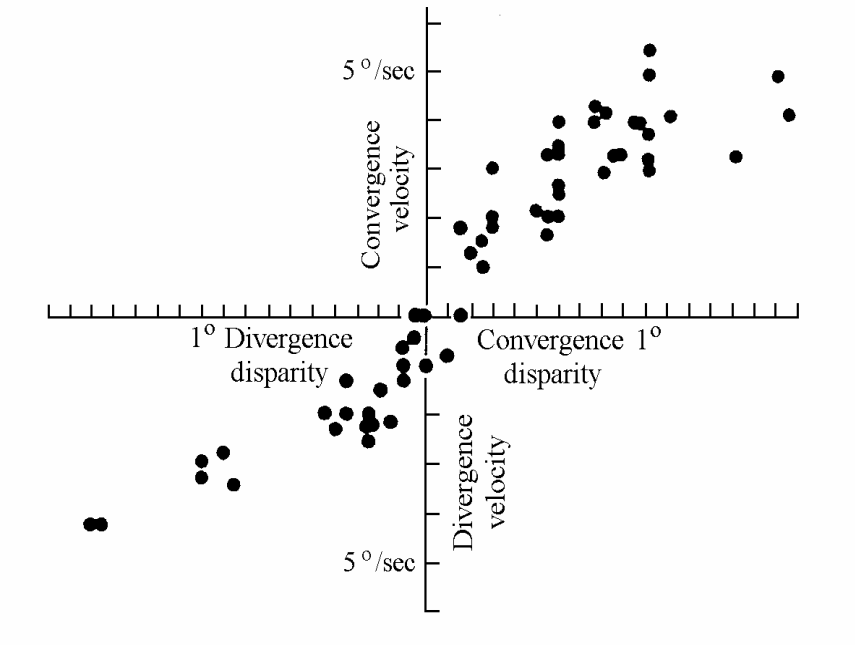

Fiigure 9.6. Ralationship between the magnitude of constantly maintained disparity and velocity of vergence response induced by it. Reprinted from Rashbass and Westheimer (1961), pg. 349, Fig. 13, with permission of The Physiological Society.

9.1.3 Basic Vergence Control Model

The basic configuration of the model of the vergence system is that of a feedback control system (described in greater detail below). It consists of a combination of dynamic elements that act in concert to accomplish an objective, i.e., bringing the images to corresponding points on the retinas to obtain sensory fusion. The model elements are designed to represent physiological components in the vergence system. The accuracy of the each model element can be confirmed by modifying its input and monitoring the output, and then comparing the resultant input-output relationship with that obtained experimentally. The model parameters can then be fine-tuned to provide a more accurate representation of vergence behavior. An important aspect of the vergence model is that of feedback control. The role of feedback control is to ensure that the output of the system attains and then maintains a desired value in the presence of variation produced by the

external environment. Mathematically, this kind of control system can be described by differential equations, in which time is the independent variable. Generally, these differential equations are transformed into the Laplace domain, where they become simple algebraic equations. The resultant solution is then inverse-Laplace transformed back into the time domain for plotting and analysis. Thus, these models provide relatively easy manipulation of the elements, and more significantly, a deeper quantitative understanding of the vergence system.

9.1.4 Overview of Chapter

This chapter is intended for the bioengineer, vision researcher, and advanced clinician working in this area. The modeling and analysis of dynamic control systems have interested engineers for many decades. In recent years, faster computers and sophisticated simulation software have enabled us to simulate complex biological systems such as the vergence system. Models of vergence and accommodation have become popular among vision scientists and clinicians because they provide useful tools for explaining the data obtained in laboratories and clinics. An example is the explanation of the discrepancy identified in the early theories of near triad control. Maddox (1886) proposed that both accommodative and vergence responses were driven primarily by blur, with the contribution from disparity being relatively small. On the other hand, Fincham and Walton (1957) suggested that disparity vergence dominated the near triad responses. Both theories were eventually subsumed after they were replaced by an interactive and comprehensive dual-feedback model (see Hung and Semmlow, 1980). We hope that continued study of the modeling of the vergence and accommodation systems will provide a better understanding of the nature of these systems.

9.2 DISPARITY VERGENCE SYSTEM MODELS

Models of vergence have been developed by various investigators to provide insight into its mechanism of control. These models are discussed below in a logical-developmental rather than chronological order.

9.2.1 Continuous Feedback Models

9.2.1.1 Rashbass and Westheimer Model

In the absence of other cues, the dominant input to the vergence control system is retinal disparity (Westheimer and Mitchell, 1956; Fincham and Walton, 1957; Stark *et al.* 1980). Binocular disparity discussed in this chapter is defined as the difference between the desired vergence angle and the actual vergence angle in the horizontal meridian of the eyes. The goal of the vergence system is to reduce the amount of retinal disparity. Thus, the system can be considered a negative feedback control system (Westheimer, 1963). Under negative feedback control with its high controller gain, the vergence response matches the vergence demand very well, with a small residual error of a few minutes of arc called "fixation disparity" (Ogle et al, 1967). Experimental results showed that vergence responses could be modified during the reaction time as well as during the vergence movement itself. This suggested that the vergence system was under continuous feedback control (Rashbass and Westheimer, 1961). However, later modeling research indicated that a "re-triggerable" discontinuous system could also produce similar pulse responses (Hung , 1998a; see below).

The first control model approximated the vergence system as a linear control system (Fig. 9.7). Rashbass and Westheimer (1961) used a ramp stimulus while holding the disparity input constant (i.e., in the open-loop

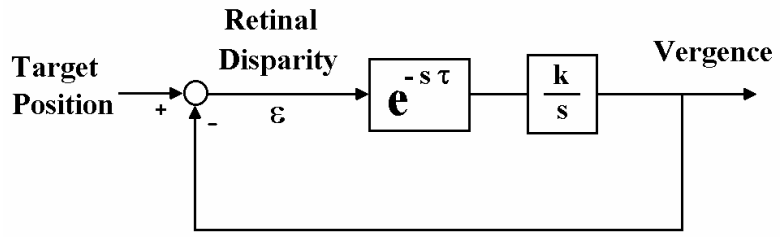

Figure 9.7. Block diagram illustrating the Rashbass and Westheimer model (1961). In this model, an integrator (k/*s*) follows a delay element ($e^{-s\tau}$). The vergence plant was assumed to have a zero-order unity gain. Disparity (ε) is the angular difference between target position and vergence position. From Patel et al (1995) with permission of the author.

condition) to study the vergence system. The advantage of operating under the open-loop condition is that it gives the experimenter complete control over the system input. They found that for small disparities up to 0.2 deg, the vergence velocity was proportional to the retinal disparity that existed one reaction time (about 160 ms) earlier (see Fig. 9.6). The following equation, then, was suggested:

$$\frac{dr}{dt} = k\varepsilon(t-\tau) \tag{9.1}$$

where r is the vergence response, ε the retinal disparity, τ the reaction time, and k the constant of proportionality. Another way to look at this equation is to convert it to the Laplace domain[1]. In this domain, Eq. 9.1 can be written as

$$sR(s) = kE(s)e^{-s\tau} \tag{9.2}$$

Under the open-loop condition, the error *E(s)* equals the input. Therefore, the forward-loop transfer function of the system, *H(s)*, is given by

$$H(s) = \frac{R(s)}{E(s)} = \frac{k}{s}e^{-\tau s} \tag{9.3}$$

Eq. 9.1 was used to predict the vergence response to an open-loop sinusoidal disparity stimulus ($\varepsilon = a\cos\omega t$). The result was that

$$r = \frac{ka}{\omega}\sin\omega(t-\tau) = \frac{ka}{\omega}\cos[\omega(t-\tau) - \frac{1}{2}\pi], \tag{9.4}$$

where a constant of integration was omitted. This result implies that if the system is linear, then a cosinusoidal disparity stimulus will evoke a sinusoidal vergence response having the same frequency as the stimulus. The vergence response will have an amplitude proportional to the amplitude of the stimulus. In addition, the gain of the system, which is defined as the ratio of the amplitude of the vergence response to the amplitude of the disparity stimulus (ka/ω in Eq. 9.4) will be inversely proportional to the frequency of the disparity stimulus. These predictions were verified by the experiment of Rashbass and Westheimer (1961). However, the prediction of the phase delay for the vergence responses to sinusoidal disparity stimuli did not agree with the experimental results. From the model, it appears that the phase lag is equal to 90^0 plus 160 ms delay. But, the measured latencies of

[1] The Laplace transform converts a differential equation for function *f(t)* to an algebraic equation for function *F(s),* in which *s* is a complex variable.

the vergence response were substantially shorter than expected. Using regular alternation of convergent and divergent step disparities, they found no reduction in phase. They therefore concluded that anticipation (i.e., prediction) did not play a role in phase reduction in the vergence system, but the system might use other information such as velocity and perhaps acceleration of the sinusoidal stimulus to reduce the phase.

9.2.1.2 Krishnan and Stark Model

Krishnan and Stark (1977) suggested a modified model that consisted of an integral-derivative controller, a time-delay element, and a third-order plant (Figure 9.8). They analyzed experimental convergence step responses and found that a parallel operator was needed; the derivative-integral element provided the fast initial response, and the "leaky" integral element (i.e., element of the form $\tau/(\tau s + 1)$, where τ is the time constant; Krishnan and Stark, 1975) provided the sustained response. The derivative element can also be thought of as a neural network that is sensitive to changes in retinal disparity rather than to the magnitude of the disparity. This parallel arrangement significantly improved the phase characteristics as compared to those of Rashbass and Westheimer.

The Krishnan and Stark model was the first to account for the difference in dynamic responses between convergence and divergence. The convergent response is generally faster than the divergent response. This represents a major non-linearity of the vergence system. Following their work, other

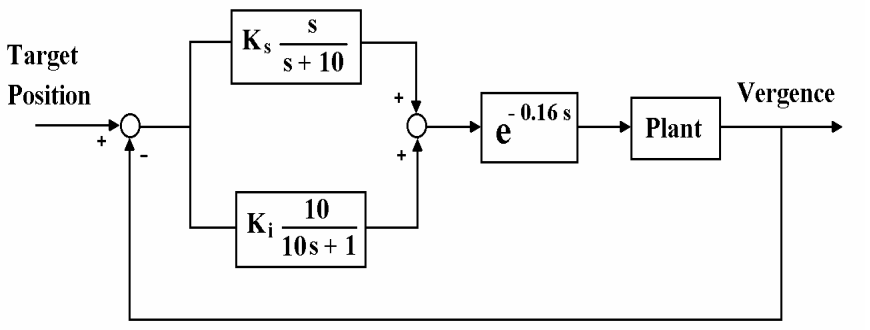

Figure 9.8. Krishnan and Stark model (1977) of the vergence system consisting of an integral-derivative controller parallel to a leaky integrator. The element $e^{-0.16s}$ represents the 160 msec delay in this system. The plant used in this model is the Cook-Stark model developed for the versional system (Cook and Stark, 1967). Reprinted from Krishnan and Stark, (1977), pg. 46, Fig. 6, with permission of © IEEE.

important non-linearity features in the vergence system, such as the saturation limits in different components and the threshold (or dead-zone) of disparity, were for the first time included in different models (Schor, 1979; Hung and Semmlow, 1980).

Under static viewing conditions (obtained by setting s = 0 in the model), the Krishnan and Stark model has a forward-loop gain of $10K_iK_p$, in which K_i represents the gain of the leaky integral controller and K_p (not shown in Fig. 9.3) represents the gain of the plant. The static gain determines the linear relationship between vergence error and the vergence response under open-loop conditions.

9.2.1.3 Schor Model

The concept of two primary control components, i.e., transient and sustained, in the vergence response was also suggested by Schor's early work (1979). However, unlike the Krishnan and Stark model, Schor used two parallel leaky integral elements for modeling the vergence controller (Figure 9.9). He simulated the vergence closed-loop response to a step stimulus. The step response of the system is the sum of the responses of the two integrators (although the output of the fast integrator is first filtered through the slow integrator; see Fig. 9.9). Schor stated that the fast integrator provided the initial step response, and then the slow integrator

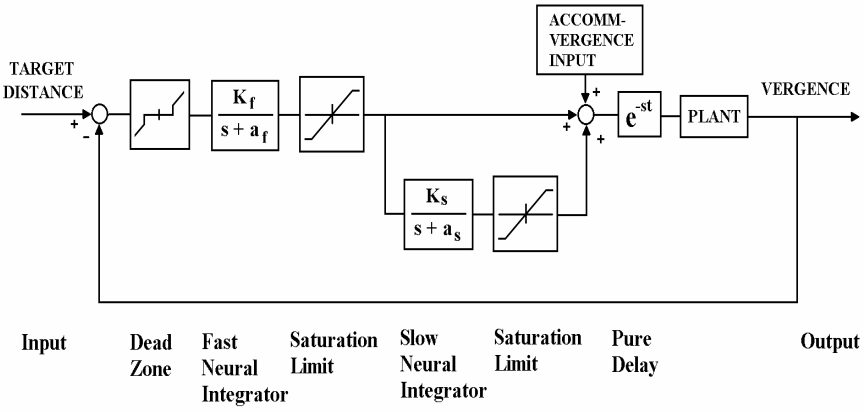

Figure 9.9. Schor model (1979) of the vergence system consisting of parallel leaky integrators. The vergence plant is assumed as a second order system. $K_f = 2.5$, $a_f = 0.1$, $K_s = 3$, $a_s = .03$, delay t is assumed to be 160 msec (not given), and dead zone limits are assumed to be ±0.25 deg (not given; although it can be shown that this has relatively little effect on the simulation responses). Reprinted from Schor (1979), pg. 834, Fig. 4, with permission of Elsevier Science.

gradually dominated the response and replaced the fast integrator drive, thus allowing it to be available for a rapid response to subsequent stimuli. In the Schor model, non-linear elements were added to represent the dead-zone and saturation limits of the fast and slow integrators.

A recent MATLAB/SIMULINK simulation of the Schor model indicated that the response to a 10 deg step stimulus consisted of large overshoot followed by oscillations over approximately the next 4 to 5 sec (Fig. 9.10). However, experimental vergence step responses did not exhibit multiple oscillations, and the step responses were completed in about 1 sec (Rashbass and Westheimer, 1961; Semmlow et al, 1986). Moreover, the duration of the oscillations in the Fast and Slow Neural Integrators were similar (Fig. 9.10), thus, calling into question the justification for distinguishing between these two components based on their dynamics.

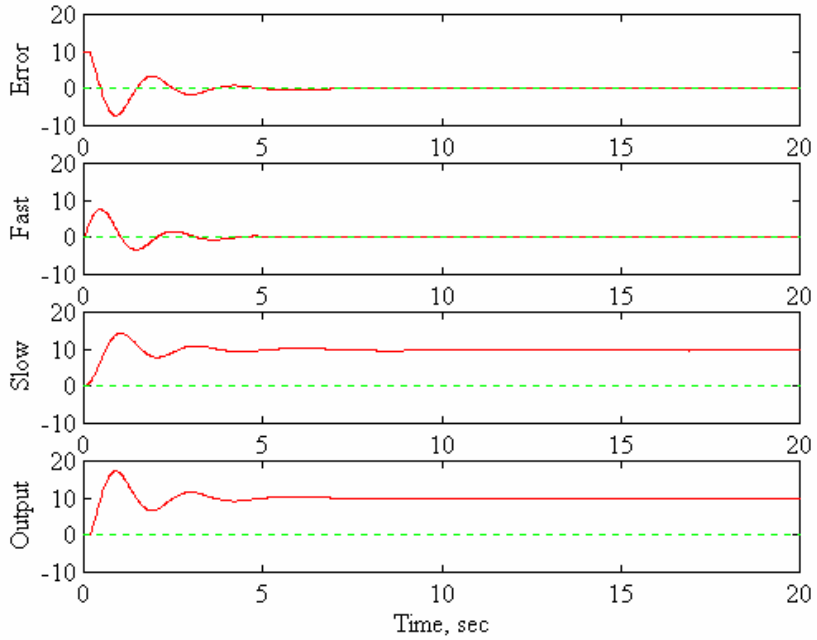

Figure 9.10. MATLAB/SIMULINK simulation of Schor's (1979) model (see Fig. 9.9) showing time courses following a 10 deg step stimulus for the vergence error, the Fast Neural Integrator output, the Slow Neural Integrator output, and the vergence response. In this simulation, the plant dynamic element (not given in the Schor model) was approximated by an all pass filter (or 1 in the Laplace domain), since it has much faster dynamics than the other forward loop elements (i.e., $1/a_f = 10$ sec, and $1/a_s = 33.3$ sec). From Hung (personal communication, 2001).

Ludvigh *et al.*(1964) presented experimental evidence to support the idea that the vergence controller has a leaky nature. In their experiment, the subject was asked to converge to a target. Then, one of his eyes was occluded (i.e., an open-loop condition for disparity vergence). Immediately after this, the vergence response started to decay to its phoria position. This provided the time constant of decay of the leaky integrator. In Schor's (1979) model, leaky integrators of the form $\tau/(\tau s + 1)$ (Krishnan and Stark, 1975) were used for the fast and slow vergence controllers. The response of a leaky integrator to a constant steady-state error input is a stable and constant vergence output. On the other hand, the response of a non-leaky (e.g., pure) integrator would be a continued integration of the constant error, resulting in an ever-growing response (Toates, 1975). Therefore, a leaky integrator is the appropriate form for the vergence controller. Moreover, non-zero fixation disparity is a necessary input signal to the controller to maintain a static vergence response under closed-loop conditions.

Schor (1979) derived an equation for the steady-state error, or fixation disparity:

$$f.\,d. = \frac{x}{kT + 1} \tag{9.5}$$

where x = vergence stimulus, k = gain of the integral controller, and T = open-loop decay time constant. However, the predicted fixation disparities based on this equation are over twice as large as those found experimentally (Schor, 1979; Hung and Semmlow, 1980).

9.2.1.4 Pobuda and Erkelens Model

Instead of using derivative-integral or leaky integral elements, Pobuda and Erkelens (1993) proposed parallel channels, each of which was sensitive to a specific range of retinal disparities with its own low-pass filter characteristics (Fig. 9.11). In each channel, the disparity signal was first selected by a range detector, and then was filtered by a correspondingly tuned low-pass filter. The output from parallel filters feeds into a slow integrator with a pure delay element (100 ms), similar to the Schor model (1979), to simulate sustained binocular fixation. A second-order low-pass filter was used to simulate the vergence plant. In their model, the open-loop phase improvement is a result of these parallel low-pass filters. However,

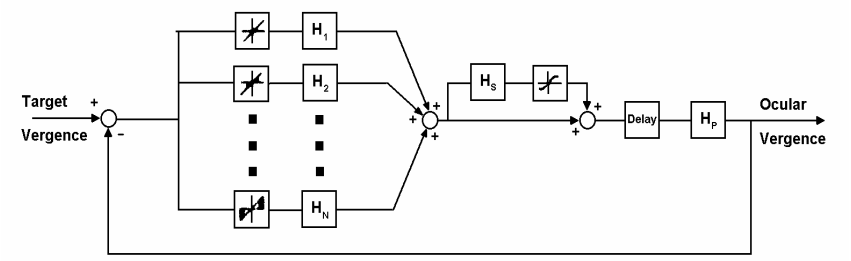

Figure 9.11. Pobuda and Erkelens model (1993) of disparity vergence. Its essential feature is the processing of disparity in several (5 were used) parallel channels, each of which is sensitive to a specific range of disparities and has its own lowpass filter characteristics (H_1, H_2, …, H_N). The model also contains a slow integrator (H_S) and a pure delay of 100 msec. The plant (H_P) is modeled by a second-order lowpass filter (i.e., a series of 2 first-order filters) with time constants of 8 and 150 msec. Reprinted from Pobuda and Erkelens (1993), pg. 227, Fig. 6, with permission of Biol. Cybernetics.

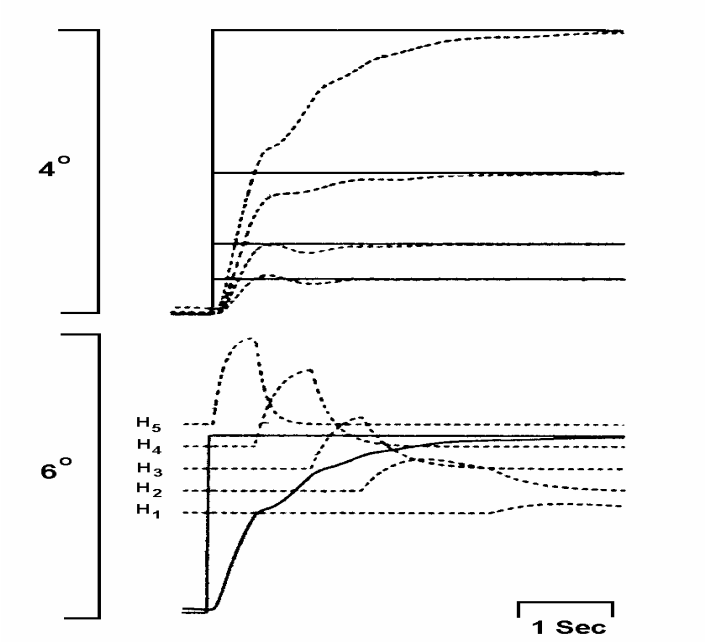

Figure 9.12. Simulation of Pobuda and Erkelens' (1993) model responses to step changes in target vergence. The upper panel shows four ocular vergence responses (dashed lines) to steps in target vergence (continuous lines) of 0.5, 1, 2, and 4 deg. The lower panel shows an ocular vergence response to a step of 4 deg in target vergence (continuous lines). The outputs of the individual lowpass filters are indicated by the dashed lines. Reprinted from Pobuda and Erkelens (1993), pg. 227, Fig. 8, with permission of Biol. Cybernetics.

model simulation step responses (Fig. 9.12) showed multiple step-like movements, which were not seen in experimental step responses such as those by Rashbass and Westheimer (1961) (Fig. 9.3). Moreover, their responses took several seconds for completion rather than one sec (Rashbass and Westheimer, 1961; Semmlow et al, 1986). This was especially evident for the larger vergence amplitudes, which were processed successively through the range of disparity filters.

9.2.1.5 Patel et al's Neural Network Model

Control theory modeling uses a "black box" approach, in which the system characteristics are derived from the relationship between the input and output of the system. For example, in the continuous vergence models discussed above (excluding Pobuda and Erkelens, 1993) and the non-continuous vergence model below (Hung et al, 1986), disparity and vergence eye-position are thought to be the input and output, respectively, without specifying how disparities are computed from retinal processing and how motoneurons are driven to generate the desired vergence response. Models built within a neural network aim to capture both the architecture and the function of the system under study, and hence overcome limitations of other models.

Patel *et al.* (1997) developed a neural network model for simulating short-term disparity vergence dynamics. The general structure of the model consists of seven functional stages as shown in Fig. 9.13. The model assumes the existence of retinotopic maps where localized and normalized activities are generated corresponding to the retinal locations of the vergence target in the two eyes. In the first stage, the localized activities in the retinotopic maps are used to detect instantaneous disparity by a pool of neurons called retinal disparity detectors. In the second stage, the detected disparities are used to generate a one-dimensional spatial map of disparity. In the third stage, the activity in the disparity map is converted to a velocity signal. The disparity encoders in the one-dimensional map activate the velocity elements with weights proportional to the encoded disparity (Rashbass and Westheimer, 1961; Krishnan and Stark, 1977). In the fourth stage, the velocity signals are converted to position signals by a push-pull architecture in which the convergence (divergence) velocity element excites the convergence (divergence) position element, and inhibits the fellow divergence (convergence) position element. The position elements are modeled as non-leaky integrators with non-linear dynamics. In the fifth stage, the position signals from the convergence and divergence position elements are converted to moto-neural activities. These moto-neural elements innervate the medial and lateral muscles of both eyes. It is important to note that in this model, the moto-neural elements also receive

inputs from the corresponding velocity elements. This velocity input plays an important role in improving the phase characteristics of the sinusoidal vergence responses. In the sixth stage, a velocity overdrive circuit with discrete parallel channels, each gated by a pre-set velocity threshold, is used to provide a velocity-dependent signal to the corresponding moto-neural element. This stage is similar to that by Pobuda and Erkelens (1993), except here velocity rather than disparity range determines the channel input that passes this stage. In the final stage, an active turn-off circuit is used to provide a discharge path for the otherwise non-leaky position elements. The discharge circuit is used to move the eyes to their tonic levels in the absence

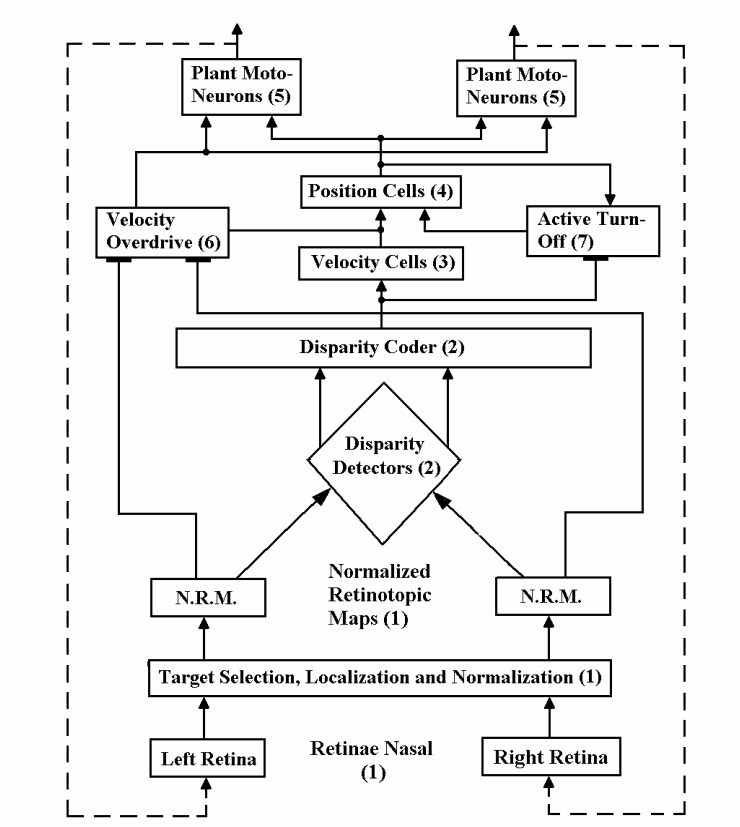

Figure 9.13 Patel *et al.* model (1997) of the vergence system. The solid lines with arrows represent the primary signal path. The solid lines with rectangular connections show modulatory signals. The dotted lines represent the external visual feedback. The numbers in the boxes correspond to those of the stages described in the text. Reprinted from Patel et al. (1997), pg. 1385, Fig. 1, with permission of Elsevier Science.

of activity in the disparity encoders. This discharge mechanism results in disassociation of the tonic vergence dynamics from the stimulus-driven dynamics. Although there is experimental evidence that velocity-driven signals contribute to the control of vergence eye movements (Mays, 1984), there is as yet no physiological evidence for the proposed velocity overdrive and velocity gate control circuits (Patel et al, 1997). Using this model, the authors simulated closed-loop (normal binocular viewing) and open loop (disparity clamped viewing) symmetric step, sinusoidal, pulse, staircase, square, and ramp wave responses. The simulation results closely resembled experimental data obtained in their laboratory and those reported in the literature (Rashbass and Westheimer, 1961; Semmlow et al, 1986, 1993; Zuber and Stark, 1968). The notable difference in their faster ramp responses (> 2 deg/sec) is that they do not exhibit the multi-step movements (which are more easily observed in the velocity traces) seen in the experimental responses (Hung et al., 1986).

9.2.2 Non-Continous Feedback Model

In contrast to continuous models, the development of the two-component (or non-continuous) theory was based on experiments that used specially-designed stimuli. For example, Westheimer and Mitchell (1956) noticed that the initial transient response amplitude could differ from that required for precise binocular fixation by as much as a degree or more. A subsequent slower movement reduced this error to attain accurate binocular fixation. Jones and Kerr (1971, 1992; Jones, 1980) used non-fusable targets, that is, a horizontal line segment presented to one eye and a vertical line segment presented to the other eye, and observed that the system initiated a transient vergence movement, with subsequent shift to the phoria or open-loop vergence position due to the lack of a fusable target. This was also shown by Semmlow et al (1986). Thus, non-fusable, dissimilar targets could initiate but not sustain the vergence response. They showed that the transient vergence component had a special property. They studied vergence responses to ramp disparity stimuli ranging from 0.7 degree/sec to 36 degree/sec with amplitudes of up to 4 degree. For lower ramp velocities (< 2 degree/sec), the vergence response consisted of a smooth following movement. Above 9 degree/sec, the vergence response was similar to a step response. When the ramp velocity was between 2 and 9 degree/sec, the vergence response consisted of a series of step responses. These small step responses had the same main sequence (peak velocity/amplitude) characteristics as the actual disparity vergence responses to step stimuli (Bahill and Stark., 1979). This result suggested a sampling and prediction

mechanism, with the system predicting the future position of the target based on stimulus velocity.

9.2.2.1 Hung, Semmlow, and Ciuffreda Model

Hung et al. (1986) developed a dual-mode model of the vergence system, which consisted of a fast open-loop component and a slow closed-loop component. The fast component had both sampling and prediction mechanisms, which provided the staircase-like step responses to fast ramp stimuli. The slow component under negative feedback control accounted for the smooth following of slowly-moving stimuli with small residual error (Figure 9.14). Simulation responses to pulse, step-pulse, ramp (Fig. 9.15), and sinusoidal (Fig. 9.16) stimuli demonstrated good fit between the simulations and experimental results. For ramp stimuli, note the multiple-step movments to faster ramp stimuli in both experimental and model simulation responses (Fig. 9.15). Also, for both step and ramp stimuli, model simulation responses exhibited faster dynamics for convergence than divergence, similar to those in experimental responses (not shown, see Hung et al, 1986, 1997). Moreover, for the sinusoidal stimuli, note the step-like responses in the higher frequencies for both experimental and model simulation responses (Fig. 9.16).

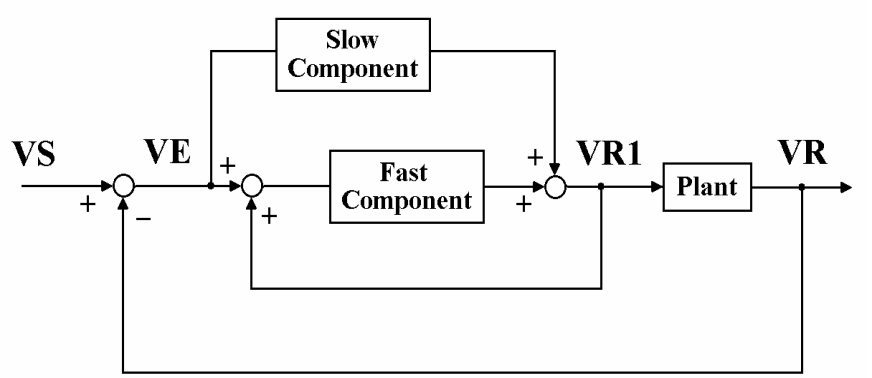

Figure 9.14. Hung *et al.* model (1986) of the vergence system. Slow and fast components are included in the forward loop of the model along with delay elements and plant. The sum of the slow and fast components, VR_1, provides a positive feedback to the fast component, as well as drives the plant. The vergence response from the plant is then compared with the vergence stimulus through the negative feedback loop to create an error signal, *VE*. Based on the VR_1, and vergence error *VE*, the fast component is able to estimate the position of target with its predictor and sampler. Reprinted from Hung et al (1986), pg. 1023, Fig. 1a, with permission of © IEEE.

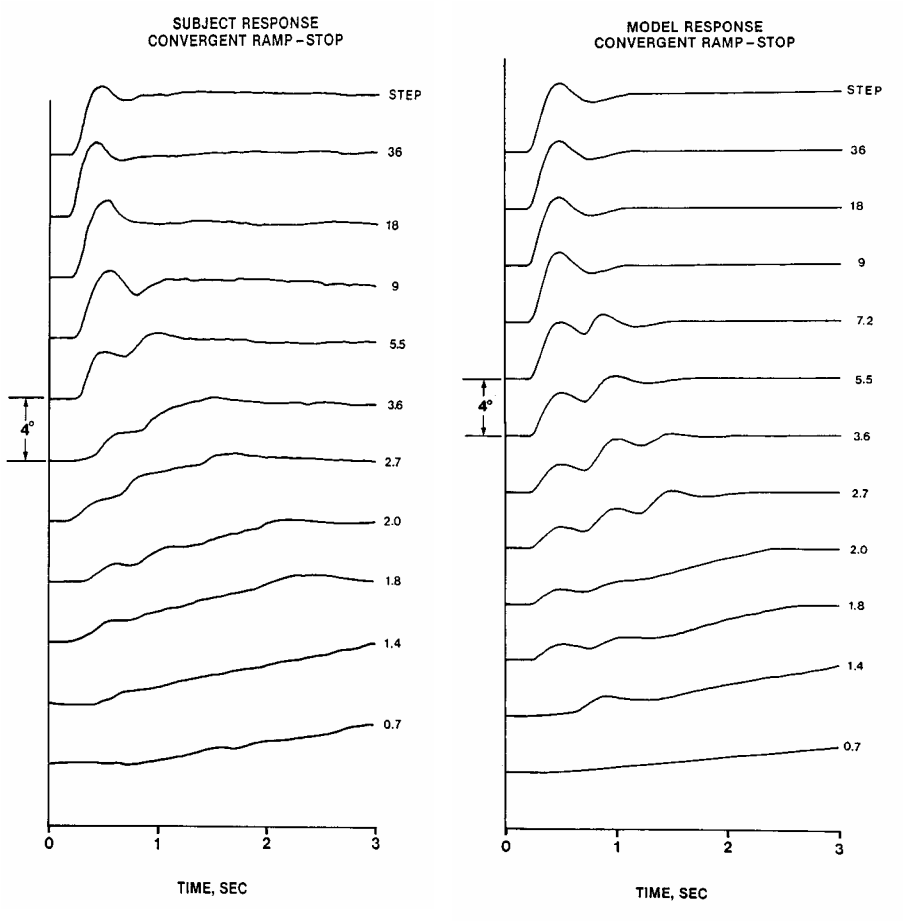

(a) (b)

Figure 9.15. Responses to convergent ramp stimuli (up to 4 deg amplitude) are shown for (a) experimental and (b) model simulation conditions. Experimental curves are individual responses. Ramp velocity, in deg/sec, is shown next to each curve. Top curves are for convergent step responses. Reprinted from Hung et al (1986), pg. 1025, Fig. 3, with permission of © IEEE.

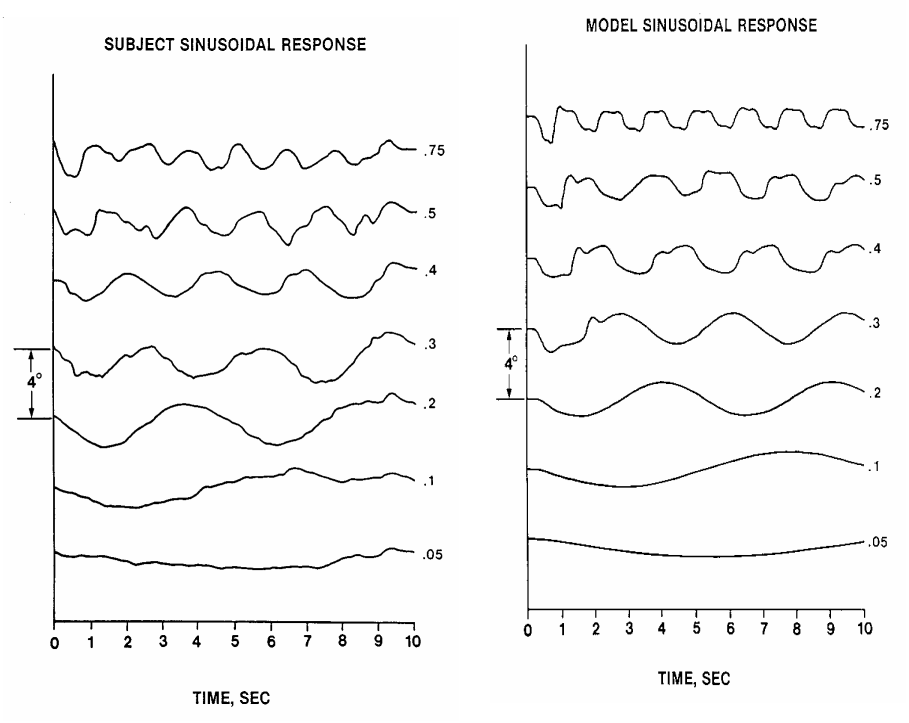

(a) (b)

Figure 9.16. Sinusoidal responses of 2 deg peak-to-peak amplitude are shown for experimental (a) and model simulation (b) conditions. Experimental curves are individual subject responses. Sinusoidal frequency of the stimulus, in Hz, is shown next to each curve. Note that for higher frequency stimulation, the model responses exhibit step-like movements similar to those in the experimental responses, which also resemble multi-step movements to faster ramp stimuli (see Fig. 9.15). Reprinted from Hung et al (1986), pg. 1026, Fig. 5, with permission of © IEEE.

9.3 ACCOMMODATION-VERGENCE INTERACTIONS

9.3.1 Cross-Links and Tonic Components

The existence of interactions between vergence and accommodation has been known at least since the work of Porterfield in 1759 (Hofstetter, 1945). Similar to the Maddox (1893) classification of vergence components, Heath (1956) suggested that there were four components in the accommodative response: blur, vergence, tonic, and proximal accommodation. After feedback control theory was used to develop models of accommodation and vergence systems (Westheimer. 1963), a basic feature of all candidate models was that blur-driven accommodation and disparity-driven vergence were controlled by two negative feedback loops. And, interactions between the two systems were represented by two feed-forward cross-links from the controller outputs, so that the accommodative controller could initiate a vergence response (accommodative vergence or AC), and conversely, the vergence controller could initiate an accommodative response (vergence accommodation or CA). The accommodative convergence/accommodation (AC/A) ratio (Fry, 1939) measures the vergence magnitude produced by a unit change in accommodation and is expressed in terms of prism diopters (or meter angles) per diopter. The convergence accommodation/convergence (CA/C) ratio (Fincham and Walton, 1957) measures the accommodation magnitude produced by a unit change in vergence and is expressed in terms of diopters per prism diopter (or meter angle).

With progress in research on the tonic positions of accommodation and vergence (Owens, 1984), these tonic components have been added to the accommodation and vergence loops to represent the stimulus-free states of each system (Hung and Semmlow, 1980). Accommodative and vergence changes and final positions in darkness are thought to represent tonic accommodation and tonic vergence, respectively (Owens and Leibowitz, 1980). However, conflicting models had been suggested as to whether the tonic elements were located before (Ebenholtz and Fisher, 1982) or after (Schor and Kotulak, 1986) inputs to the feed-forward cross-links. If both reflex and tonic component signals arrived before the cross-links and drove the complementary system, then the accommodative (or vergence) response measured under the dual open-loop condition would represent not only a part of its own system's tonic level, but also a portion of the tonic vergence (tonic accommodation) as relayed by the cross-link. However, this was not seen experimentally. For example, Jiang (1996) found experimentally that higher dark focus (i.e., tonic values obtained in darkness) values were associated with lower, rather than higher, near dissociated phorias. This result suggested that the tonic elements were located after the cross-links.

Therefore, the values of accommodation and vergence with both feedback loops opened represent the tonic positions of the two systems.

9.3.2 Static Interactions Between Accommodation and Vergence

9.3.2.1 Hung and Semmlow Model

Hung and Semmlow (1980) suggested a model to simulate quantitatively the static behavior of accommodation and vergence. A block diagram of this model is shown in Fig. 9.17. The difference between the accommodative stimulus (AS) and the accommodative response (AR) forms the accommodative error (AE), or defocus, signal. To drive the accommodative controller, this error signal first has to pass a deadspace (DSP), a non-linear threshold element. The accommodative controller has a gain ACG. This static gain is based on the assumption that the accommodative system has an open-loop transfer function $ACG/(\tau s+1)$ as a first-order system. The output from the accommodative controller is summed with tonic accommodation (ABIAS) and vergence accommodation at a summing junction, and also provides an accommodative vergence signal to the vergence system through the cross-link. The output from the summing junction goes through a saturation element, which simulates the accommodative plant, to provide the

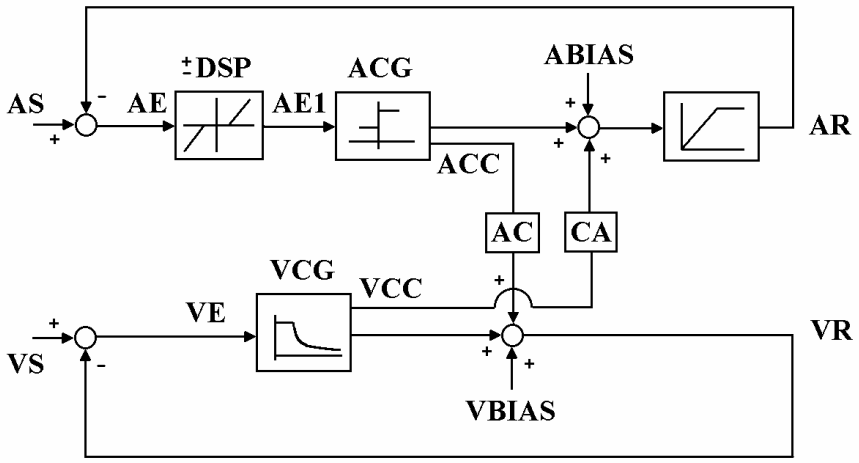

Figure 9.17 Hung and Semmlow (1980) model of the static interactive dual feedback accommodation and vergence systems. Reprinted from Hung and Semmlow (1980), pg. 441, Fig. 1, with permission of © IEEE.

accommodative response (AR). The difference between the vergence stimulus (VS) and the vergence response (VR) is the vergence error (VE). Static vergence error is referred to as fixation disparity under binocular viewing conditions. Vergence error goes through a vergence controller with gain VCG. The output from the vergence controller is summed with tonic vergence (VBIAS) and accommodative vergence to drive the vergence plant (omitted in the model) and provide the vergence response (VR). The cross-links receive a signal from one system's controller and link to another system at the point between the controller and tonic component with a gain AC or CA. Here, the gains AC and CA are proportional to AC/A and CA/C ratios, respectively, (see Hung and Semmlow, 1982).

The Hung and Semmlow model is concerned with short-term static responses. They demonstrated the ability of the model to predict human static near response behavior under various circumstances (Hung and Semmlow, 1980). They also investigated the controller sensitivities of accommodation and vergence to changes in stimulus (Hung and Semmlow, 1982). The results indicated that the contributions of the outputs of the accommodation and vergence controllers to accommodative and vergence responses in normal binocular vision were dependent on the individual's cross-link parameters, i.e. the AC and CA values. This suggested that normal AC and CA values lay in a continuum between the two extremes of accommodative-dominated (Maddox, 1893) and vergence-dominated (Fincham-Walton, 1957) control. This study (Hung and Semmlow, 1982) also indicated that the stability of the model (Hung and Semmlow, 1980) required the term $(1+ACG)(1+VCG)-AC*CA*ACG*VCG$ to not equal zero. When ACG and VCG are high enough to have $ACG \cong 1+ACG$ *and* $VCG \cong 1+VCG$, this stability requirement suggests that AC and CA should not be reciprocals of each other in subjects with normal binocular vision. More recent research has demonstrated that they have an inverse but not reciprocal relationship (Rosenfield et al, 1995).

It can be shown that under the open-loop vergence condition, the accommodative response AR, accommodative controller output ACC, and vergence response VR are given by (Hung and Semmlow, 1980):

$$AR = (AS \mp DSP) * \frac{ACG}{1+ACG} + ABIAS * \frac{1}{1+ACG} \tag{9.6}$$

$$ACC = (AS \mp DSP - ABIAS) * \frac{ACG}{1+ACG} \tag{9.7}$$

and

$$VR = AC * ACC + VBIAS \tag{9.8a}$$

or

$$VR = AC * (AS \mp DSP - ABIAS) * \frac{ACG}{1 + ACG} + VBIAS \tag{9.8b}$$

9.3.2.2 Jiang and Woessner Analysis of the Hung and Semmlow Model

Jiang and Woessner (1996) defined AR_0 and VR_o as the accommodative and vergence responses, respectively, under the vergence open-loop condition and for AS = 0. Thus, from Eq. 9.6,

$$AR_0 = (\mp DSP) * \frac{ACG}{1 + ACG} + ABIAS * \frac{1}{1 + ACG} \tag{9.9}$$

and from Eqs. 9.8b,

$$VR_0 = AC * (\mp DSP - ABIAS) * \frac{ACG}{1 + ACG} + VBIAS \tag{9.10}$$

It can be shown that by substituting Eqs. 9.6, 9.9 and 9.10 into Eq. 9.8b, and re-arranging, we obtain

$$VR = AC * (AR - AR_0) + VR_0 \tag{9.11}$$

Jiang and Woessner (1996) also sought to find the open-loop vergence response for the specific condition on the AS/R curve when

$$AR=ABIAS \tag{9.12}$$

Substituting Eq. 9.12 into Eq. 9.6 and rearranging gives

$$ABIAS = AS \mp DSP \tag{9.13}$$

Substituting Eq. 9.13 into Eq. 9.7 results in an accommodative controller output (ACC) value of zero, which is normally associated with open-loop of accommodation. However, the above equations are based on closed-loop of accommodation. A possible solution to this dilemma is that the accommodation system, under the conditions of AR=ABIAS and open-loop vergence, may operate just at the boundary between being open- and closed-

loop (and eventually settling on the nearest closed-loop value). Thus, greater variability would be expected under this condition. Supportive evidence for this can be seen in the data of Kotulak and Schor (1968b; pg. 226, Fig. 4), which showed in 2 of 3 monocularly viewing subjects a slightly larger accommodative variability for a stimulus near the subject's tonic level.

The zero ACC value results in a zero crosslink drive, and thus VBIAS is the only remaining drive of vergence (see model, Fig. 9.17). Indeed, substituting Eq. 9.13 into Eq. 9.8b gives

$$VR = VBIAS \tag{9.14}$$

Substituting Eqs. 9.12 and 9.13 into Eq. 9.11 gives

$$VBIAS = AC * (ABIAS - AR_0) + VR_0 \tag{9.15}$$

Using the more descriptive terms tonic vergence (TV) for VBIAS, and tonic accommodation (TA) for ABIAS, and also calling VR_0 the distance heterophoria (Jiang and Woessner, 1996), the equation becomes

$$TV = AC/A * (TA - AR_0) + \text{distance heterophoria.} \tag{9.16}$$

The authors experimentally verified this equation. Before this study, O'Shea *et al.* (1988) and Wolf *et al*. (1990) predicted the TV from measurements of the TA, the distance heterophoria, and the AC/A ratio; Owens and Tyrrell (1992) predicted the distance heterophoria from measurements of the TV, the AC/A ratio, and the accommodative relaxation from the TA to the distant target. The Jiang and Woessner (1996) study extended the results of these studies to a general situation and gave these results a uniform explanation.

9.3.2.3 Sensitivity Analysis of Relative Accommodation and Vergence

To investigate the effect of parameter variation on accommodative and vergence responses, a sensitivity analysis was performed on the static dual-interactive model (Hung and Ciuffreda, 1994). Model simulation responses were computed under two conditions using parameter values obtained in a previous study (Hung and Semmlow, 1980). The first condition was to calculate the accommodative error when the accommodative demand was systematically varied between ± 2.5 D, while the vergence demand was held at 2.5 MA. The second condition was to calculate the vergence error when

the vergence demand was systematically varied between 25 BI and 25 BO, while the accommodative demand was held at 2.5 D. Moreover, each parameter was repeated at 50% and 150% of the nominal value, while all other parameters were held constant at their nominal values.

The results indicated that the model was most sensitive to variations in the cross-link gains AC and CA. These gain elements interconnect the two feedback systems, and thus determine the extent of mutual interaction between accommodation and vergence. Since the output from each controller is multiplied with its cross-link gain element to serve as an input to the fellow system, it effectively increases these interactive influences. That is, the multiplicative effects of each parameter, both within and across each motor system, contribute to and therefore influence the overall response to achieve steady-state system stability. It can be shown (Hung and Ciuffreda, 1994) that the main effect of increased AC or CA is to increase the accommodative and vergence errors, with this occurring to a much greater extent than from variation in the other parameters. Moreover, high AC and CA values may lead to instability in the interactive system and result in abnormalities such as strabismus (Hung and Semmlow, 1982)

On the other hand, it was found that the model was only moderately sensitive to variations in the controller gains ACG and VCG. This can be explained by the fact that for an isolated feedback control system, the overall closed-loop gain attributed to the controller is of the form G/(1+G). Such a closed-loop term is inherently only moderately sensitive to changes in G. Indeed, it is a basic feature of a negative feedback system to maintain stability despite larger fluctuations in the controller gain. In addition, since each controller primarily governs its own feedback loop and has only an indirect influence on the fellow loop, changes in gain would have a relatively small influence on the fellow system's response. However, low controller gain values, such as a low ACG, may be associated with central deficits such as amblyopia and congenital nystagmus (Hung and Semmlow, 1982; Hung and Ciuffreda, 1994).

Also, the model was only moderately sensitive to changes in the tonic terms ABIAS and VBIAS, and was quite insensitive to variations in the deadspace elements. This is in agreement with earlier experimental results (Ogle, 1972; Ogle, *et al.*, 1967; Ripps *et al.*, 1962).

Blackie and Howland (2000) used a state-space technique (i.e., a derivative-based simultaneous-equation mathematical approach) to performed a stability analysis of the Hung and Semmlow (1980) model. Consistent with Hung and Semmlow's (1982) earlier results, they found that the dual-interactive feedback system became unstable when the product AC*CA was greater than one.

9.3.2.4 Deadspace, a Nonlinear Element in the Accommodation System Model

The deadspace (DSP) in the control theory model of accommodation represents the depth-of-focus of the eye (Hung and Semmlow, 1980). Kotulak and Schor (1986a) found that the defocus threshold for eliciting a motor response from accommodation was about 0.12 – 0.14 D. Based on this result, Schor (1992) suggested that the value of DSP (or threshold) in his model should be much smaller than the depth-of-focus. Hung and Ciuffreda (1994) called the threshold measured with the Kotulak and Schor method (or a similar method) the "objective threshold", and they called the threshold based on the probability of detection the "subjective threshold". In reviewing previous studies, they found that the subjective-threshold was consistently larger than the objective-threshold. Mordi and Ciuffreda (1998; Mordi, 1991; Ciuffreda et al, 2000) confirmed this finding, and moreover extended it to show that the subjective threshold increased with age whereas the objective threshold did not.

In the case where vision is not normal (i.e., worse than 20/20 visual acuity), the effective threshold for the depth-of-focus may increase. To investigate this quantitatively, Jiang (2000a,b) modified the deadspace element in the Hung and Semmlow (1980) model. He first clarified the definitions of different defocus thresholds and discussed the differences between these thresholds. The depth-of-focus of the human eye is not only related to the optical system of the eye, but also the sensory system of the eye. Quantitatively, the depth-of-focus can be estimated by using both geometric and physical optics methods (Green, *et al.*, 1980). One equation is:

$$\Delta D = 17.45\phi / p, \tag{9.17}$$

where ΔD is the depth-of-focus in diopters, p the pupil diameter in millimeters, and ϕ the minimal resolvable angle in degrees. This equation shows that the depth-of-focus is related to both pupil size and visual resolution of the eye. Jiang (2000a,b) suggested naming the depth-of-focus measured with a psychophysical procedure the "perceptual defocus threshold" (i.e., the subjective-threshold in the previous example) to distinguish it from the depth-of-focus estimated from the above equation. The depth-of-focus or perceptual-defocus-threshold was thought to be the non-linear operator (DSP) in control theory models that simulate the static behavior of accommodation (e.g., Hung and Semmlow, 1980). Any defocus signal has to be larger than DSP to drive the controller and change the accommodative response. Based on these models, DSP does not affect the slope of the accommodative response function, which is only determined by

the gain of the accommodative controller (ACG). However, not all changes in the slope of the AS/R function are related to changes in the ACG alone. For example, when the pupil size becomes very small (≤ 1 mm), the accommodative feedback loop is opened, and the slope of the AS/R function becomes flat. In this case, the only change is an increase in the optical depth-of-focus. Jiang (1997) suggested adding a linear operator with gain ASG (accommodative sensory gain) in front of DSP to account for the sensory performance of the accommodative system (see accommodation model in Chap. 8 of this volume). From this model, he derived the following equation:

$$AR = K * (AS - \frac{DSP}{ASG}) + (1 - K) * ABIAS \qquad (9.18)$$

where AS is the accommodative stimulus, AR the accommodative response, ABIAS the tonic accommodation, and K (= (ASG*ACG)/(1+ASG*ACG)) the slope of the AS/R function. These parameters can be measured experimentally. The ratio (DSP/ASG) serves the same role as DSP in the Hung and Semmlow (1980) model, and represents the amount of retinal defocus signal (error) needed by the accommodative system to maintain the static response. Jiang and his co-workers found that this threshold for emmetropic subjects was about 0.40–0.45 D and for myopic subjects, whose refractive errors were progressing, was about 0.78-0.88 D (Jiang, 1997; Jiang and Morse, 1999). Jiang (2000a,b) named this the sensory-motor threshold.

He defined the "accommodative stimulus/response (AS/R)", threshold as the smallest change in accommodative stimulus that creates a detectable change in accommodative response (i.e., the objective-threshold; Mordi, 1991; Mordi and Ciuffreda, 1998). This objective threshold is different from the subjective perceptual-defocus threshold because it depends on the accommodative response instead of the subjectively perceived blur (Hung and Ciuffreda, 1994). From the modified model (see Eq. 9.17; Jiang, 1997), it can be seen that the change in response depends only on the change in stimulus and the slope of the accommodative AS/R function, i.e. that

$$\Delta AR = K\Delta AS, \qquad (9.19)$$

where Δ represents a change. In support of this, Winn et al. (1989) had shown that the threshold for the detection of defocus was close to the root-mean-square (r.m.s.) value of the accommodative microfluctuations. Their result suggested that the change of accommodative response must be larger than the intrinsic noise level of the system for it to be detected. Also, Wong and Jiang (2000a,b) found a high correlation between the AS/R threshold and the average standard deviation of the accommodative response measurements among 36 subjects ($r = 0.70$, $p < 0.005$).

Jiang's distinction between these thresholds is supported by the finding that the AS/R threshold (i.e., the objective threshold) is smaller than the perceptual-defocus threshold (i.e., the subjective threshold) (Mordi and Ciuffreda, 1998). Moreover, the objective threshold was found to be unchanged with age, whereas the subjective threshold increased at a rate of 0.027 D/year (Mordi and Ciuffreda, 1998). These results indicate that the oculomotor mechanism associated with the objective threshold is different from the perceptual-defocus process associated with the subjective threshold.

9.3.2.5 Hung, Ciuffreda, and Rosenfield Proximal Model of Accommodation and Vergence

The Hung et al (1996) proximal model of accommodation and vergence is shown in Fig. 9.18. For the first time, it takes into account the contribution of proximity, or awareness of nearness (Toates, 1974; Maddox, 1893), on the total system steady-state response. The positions of the components in the model were based on open- and closed-loop accommodative and vergence experimental results (Hung and Semmlow, 1980; Fisher, 1988; Rosenfield and Gilmartin, 1990; Rosenfield et al, 1991).

The interactive model equations were solved in the form of a ratio between proximal contribution and either the overall accommodative or vergence response. It was found that the relative contribution of proximal accommodation to the overall accommodative response under accommodation CL and vergence OL was given by:

$$\left[\frac{\text{Proximal Accommodation Term}}{\text{Overall Accommodative Response}}\right]_{\text{Acl, Vol}} = \frac{0.0409 * \text{DS}}{0.950 * \text{DS} + 0.0555} \tag{9.20}$$

where DS is the distance stimulus. Also, the relative contribution of proximal accommodation to the overall accommodative response under accommodation CL and vergence CL was given by:

$$\left[\frac{\text{Proximal Accommodation Term}}{\text{Overall Accommodative Response}}\right]_{\text{Acl, Vcl}} \tag{9.21}$$

$$= \frac{[\text{APG} * (1 + \text{VCG}) - \text{APG} * \text{VCG} * \text{AC} * \text{CA} + \text{VPG} * \text{CA}] * \text{PDG} * \text{DS}}{[\text{ACG} * (1 + \text{VCG}) - \text{ACG} * \text{VCG} * \text{AC} * \text{CA}] * \text{AS} + \text{VCG} * \text{CA} * \text{VS}}$$

$$+ [\text{APG} * (1 + \text{VCG}) - \text{APG}*\text{VCG}*\text{AC}*\text{CA} + \text{VPG}*\text{CA}] * \text{PDG} * \text{DS}$$

$$+ (1 + \text{VCG}) * \text{ABIAS} - \text{VCG} * \text{CA} * \text{VBIAS}$$

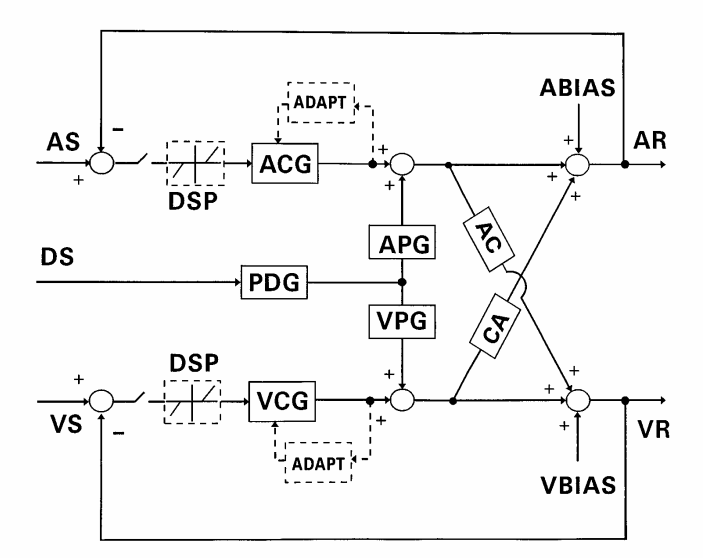

Figure 9.18. Hung, Ciuffreda, and Rosenfield (1996) proximal model of accommodation and vergence. Most of the model parameters are the same as those in Fig. 9.17. For the proximal components, the distance stimulus (DS) is input to the perceived distance gain (PDG) element, which represents the subjective apparent distance estimate. It then goes through the accommodative proximal gain (APG) and vergence proximal gain (VPG) elements, which represent the contribution from target proximity to the two systems, respectively. Moreover, the outputs of these elements are summed with ACG and VCG, respectively, and the summed signals proceed in the forward-loop paths. The adaptation component (ADAPT) is shown in this static model for completeness only. Reprinted from Hung et al (1996), pg. 32, Fig. 1, with permission of Elsevier Science.

Similar expressions were obtained for the vergence contribution under the different conditions. The definition of the parameters and their nominal values are given in Table 9.1. Upon substitution of the parameter values from Table 9.1 into the model equations, it was found that under the dual open-loop (OL) condition, the contribution of proximal accommodation (PA) to the overall accommodative output ranged from 42.5 to 81.6%, whereas the contribution of proximal vergence (PV) to the overall vergence output ranged from 56.1 to 88.5%. In contrast, under nearly all other stimulus conditions, the relative contributions were much smaller, ranging from 0.04 to 7.0%. These results are consistent with experimental and clinical findings (Hokoda and Ciuffreda, 1983; Wick, 1985; and North et al, 1993). Thus, although the relative contributions of PA and PV were large under the dual-OL condition, they were generally very small under the various closed-

loop conditions that simulated more naturalistic viewing situations. Nevertheless, Hung et al (1996) suggested that proximity still plays an important role, with these cues reinforcing the dominant blur and disparity motor responses.

Table 9.1 - Proximal Model Parameter Values

Reprinted from Hung et al (1996), pg. 34, Table 1, with permission of Elsevier Science.

Perceived Distance Gain	PDG	0.212
Accommodative Proximal Gain	APG	2.100
Vergence Proximal Gain	VPG	0.067
Accommodative Controller Gain	ACG	10.0
Vergence Controller Gain	VCG	150.0
Accommodative Convergence	AC	0.80 MA/D
Convergence Accommodation	CA	0.37 D/MA
Tonic Accommodation	ABIAS	0.61 D
Tonic Vergence	VBIAS	0.29 MA

9.3.2.6 Eadie, Carlin, and Gray Fuzzy Set Model of Accommodation and Vergence

Eadie et al. (1999) applied a fuzzy set approach to represent the accommodative and vergence proximal gain elements such as those in Fig. 9.18 (see Fig. 9.19). Fuzzy logic control is a mapping procedure which relates the input to the output using a fuzzy set (Zadeh, 1965, 1994). A list of "If… then…" statements define the fuzzy set. For example: "If distance is far, then proximal accommodation is low; If distance is near, then proximal accommodation is high." The relative impreciseness, or fuzziness, of the input-output relationship provides a response characteristic, over the range of normal response variability, that is meant to be a more realistic representation of the actual physiological control process. Their simulation responses showed that the proximal contribution was high under the dual open-loop condition, but was negligible under the dual closed-loop condition, similar to that found previously by Hung et al. (1996).

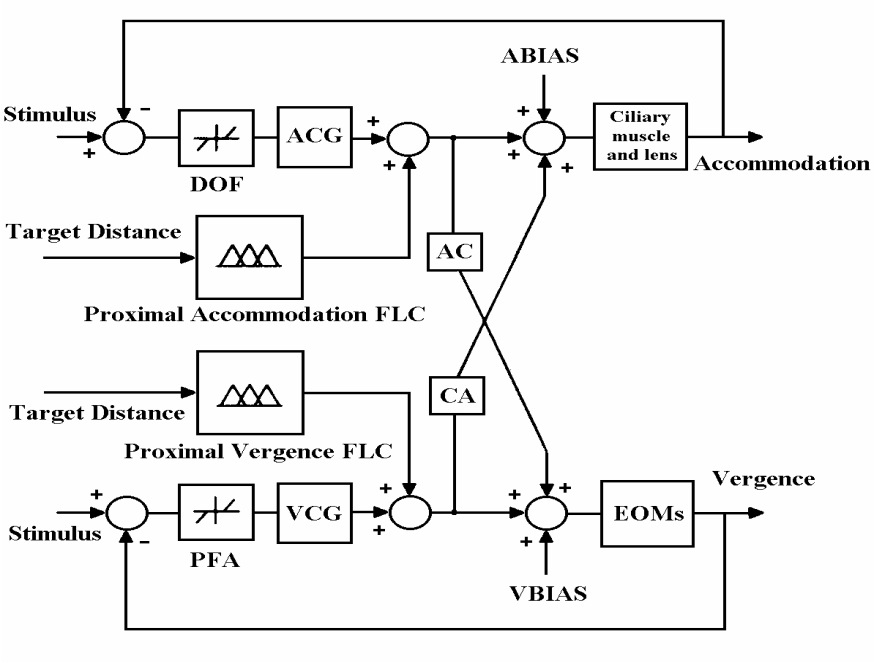

Figure 9.19. Eadie, Carlin, and Gray (1999) fuzzy set model of accommodation and vergence. Most of the model parameters are the same as those in Fig. 9.18. Proximal accommodation and vergence fuzzy logic control (FLC) replace PDG*AGP and PDG*VPG in Fig. 9.18. Reprinted from Eadie et al. (1999), pg. 179, Fig. 1, with permission of Plenum Press.

9.3.3 Dynamic Interactions Between Accommodation and Vergence

9.3.3.1 Schor Model

In 1992, Schor developed his dynamic model of the interaction between accommodation and vergence (Fig. 9.20). This model differed from his previous model (Schor, 1979) in that, in the fast component part of this model, an additional proportional gain path (K_b) was added in parallel with the leaky integrator to provide a fast-slow combination for the phasic response. But as the simulation of his earlier model showed (see above), this may not actually provide a fast-slow combination of movements in the response. The output clipper element for the fast integrator in the previous model was removed. In the slow component part, the saturation limit non-

linear element, located after the slow integrator, remained. A non-linear filter that served as a stimulus funnel was added to limit the input to the slow integrator. Both the fast and slow components used leaky integrators. These integrators were characterized by their gains (*K*) and decay time constants (*1/a*). In the plant part, the new model used first-order control elements for both accommodation and vergence plant mechanisms. The configuration and parameters of this model were justified based upon his observations of the dynamic behavior of accommodation, vergence, and their cross-link interactions (Schor, 1992). In contrast to the static models (Hung and Semmlow, 1980; Schor, 1985), this model has only unity-gain elements in the cross-links. However, Schor (1999) recently has added non unity-gain AC/A and CA/C elements into the cross-links of his model.

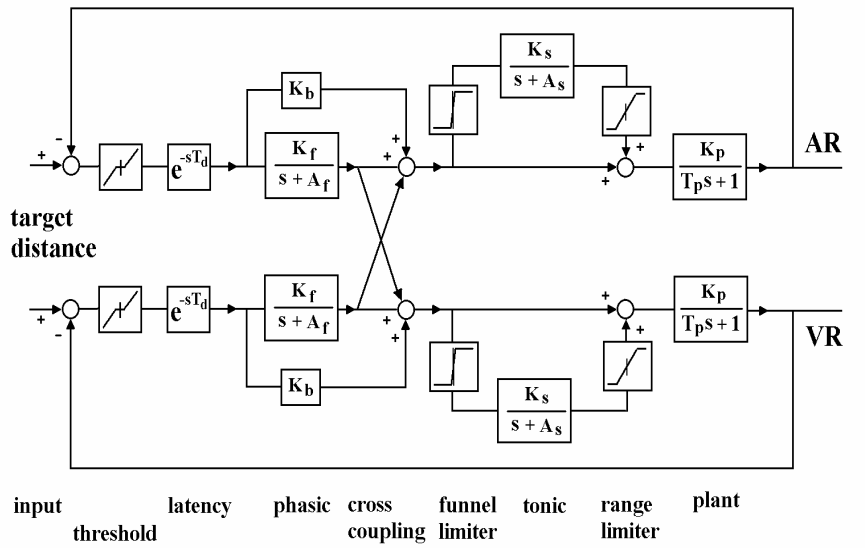

Figure 9.20. Schor (1992) dynamic interactive model of accommodation and vergence. This model includes phasic and tonic control components. In the tonic component, signal passes a funnel limiter first before it reaches the tonic integrator, then the signal is limited by a saturation limiter. Both limiters are non-linear elements in the model. Reprinted from Schor (1992), pg. 261, Fig. 1, with permission of Optom. Vis. Sci.

Schor's model simulation closed-loop step responses are shown for accommodation and vergence in Fig. 9.21. The vergence responses exhibit high frequency oscillations. Although Schor claims that these high frequency oscillations are a characteristic of the closed-loop step response (Schor, 1992), they are not observed experimentally (Rashbass and Westheimer, 1961; Hung et al, 1986; see Figs. 9.3 and the step response in Fig. 9.15). Moreover, no pulse, ramp or sinusoidal simulations were presented.

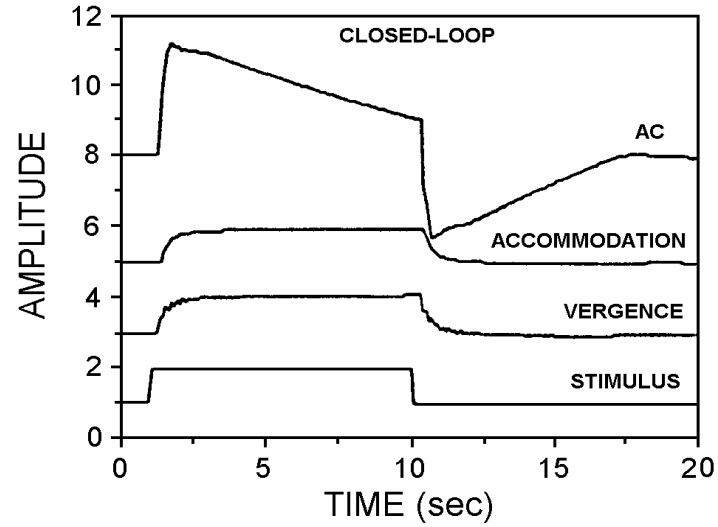

Figure 9.21. Schor (1992) model simulation of closed-loop step responses for accommodation and vergence. Also shown is the accommodative convergence drive (AC). Note the rapid oscillations in the vergence response, which is not seen experimentally (Rashbass and Westheimer, 1961; see Fig 9.3). Reprinted from Schor (1992), pg. 263, Fig. 2, with permission of Optom. Vis. Sci.

9.4 ADAPTATION MODELS OF ACCOMMODATION AND VERGENCE

Both accommodation and vergence have been shown to exhibit adaptation after extended near viewing. Normally, when the stimulus to accommodation is removed, the accommodation system returns rapidly towards its tonic position. However, if the stimulus is removed after sustained focusing effort, the decay is much slower, and in some cases the initial steady-state level is directionally biased for a substantial period of

time. A similar effect can be observed in the vergence system. For example, after prolonged wearing of horizontal prisms, occlusion of one eye results in a much slower decay of the vergence output towards its tonic value.

9.4.1 Schor Model

In the slow component of his model, Schor (1992) used a leaky integrator with two non-linear elements, a funnel limiter and a range limiter, to simulate the adaptive process. Patel (1995) used the vergence part of this model (Schor, 1992) to simulate the open-loop response and found that if a constant disparity of 0.1 MA were held for 20 seconds, the vergence output would saturate at 1.25 MA in conjunction with the vergence velocity signal decaying to zero. If the disparity stimulus were 1 MA, then the open-loop response would saturate at about 4.5 MA. However, this saturating phenomenon in the simulations is not consistent with experimental observation. Furthermore, Hung (1992b) investigated the overall transfer function of Schor's model and found that the form of the transfer function did not exhibit adaptive properties.

9.4.2 Hung Model

Hung (1992b) developed a model to simulate accommodative and vergence adaptive responses. The model was based on the static dual-interactive model of the accommodation and vergence systems (Hung and Semmlow, 1980). The components of the basic accommodation and vergence systems are similar. Both contain a controller in the forward-loop. The controller consists of a fast and a slow component. The fast component drives the initial dynamic portion of the response, whereas the slow component maintains closed-loop feedback of the steady-state level (Westheimer and Mitchell, 1956; Jones, 1980; Hung and Ciuffreda, 1988). The tonic component represents the value of accommodation or vergence when the feedback loop is opened (Toates, 1972; Hung and Semmlow, 1980). To account for the change in decay characteristics following sustained fixation, an adaptive component is incorporated which receives its input from the output of the controller. This is consistent with the concept that adaptation is related to the effort of accommodation or vergence (Hung, 1998b). Neurologically, adaptation may take place in the cerebellum (Windhorst, 1999) in response to the sustained effort, which in turn modifies the neural integrator circuitry controlling the oculomotor system. The unique feature of the model is that the sustained element time constant is modified by the adaptive component output. Thus, in the accommodation and vergence sub-systems, as the controller output increases with increased effort, the adaptive component increases the time constant of the sustained

element. If at that point the feedback loop is opened, the decay of the sustained element will take longer, thereby simulating the longer decay time following prolonged adaptation found experimentally.

The combined accommodation and vergence adaptation model is shown in Fig. 9.22 (Hung, 1992b). Consider first the accommodative loop. The deadspace element (DE) represents the neuro-optical depth-of-focus. The controller output is multiplied by factor m_A and input to a tanh function, which serves as a compression element (CE). The factor m_A is used to provide an appropriate range on the abscissa of the tanh function. The compression element reduces the controller output for large magnitude inputs, so that the adaptation effect is not drastically different at various adapting stimulus levels. The adaptive component is represented by the first-order dynamic element

$$\frac{1}{T_{A1}s+1} \tag{9.22}$$

where T_{A1} is the time constant of accommodative adaptation. The accommodative adaptation gain, K_A, controls the magnitude of the adaptive

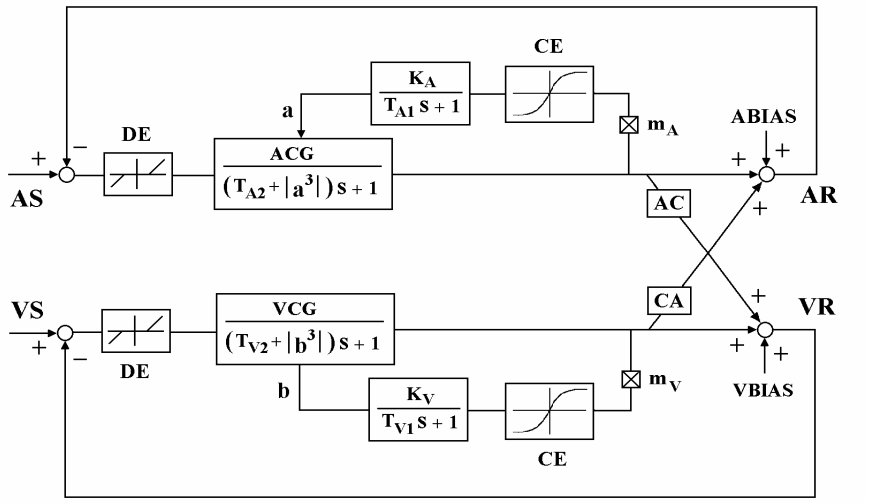

Figure 9.22. Hung (1992b) adaptation model of combined accommodation and vergence system. The time constants T_{A2} and T_{V2} of the accommodative and vergence controllers, respectively, are modified by their adaptive components. In each feedback loop, the adaptive component consists of a constant gain (m_A or m_V) element, a compression element (CE), and a first-order dynamic controller. Reprinted from Hung (1992b), pg. 322, Fig. 3, with permission of Elsevier Science.

component output level. The adaptive element output, *a*, modifies the time constant of the accommodative controller via the term

$$T_{A2} + \left| a^3 \right| \tag{9.23}$$

where T_{A2} is the fixed portion of the time constant. The cubic relationship was obtained empirically to provide a negligible increase in the time constant for a small amount of adaptation, but a very long time constant for a large amount of adaptation. A similar configuration applies to the vergence system, where the deadspace element (DE) represents Panum's fusional area. The vergence adaptive component consists of multiplier *m,* compression element CE, adaptive gain K_V, adaptive time constant T_{V1}, adaptive element output *b*, and controller time constant $T_{V2} + \left| b^3 \right|$.

A number of adaptation experimental results (Henson and North, 1980; Sethi and North, 1987) were accurately simulated using parameter values of the subjects in a previous study (Hung, 1992b). The adaptation simulation results can also explain how accommodative hysteresis occurs. Following sustained near viewing, the adaptive element output remains high as it begins its decay towards the tonic level, or ABIAS. Hence, immediate post-task accommodative response measured in the dark is higher than the tonic value. On the other hand, following sustained far viewing, the adaptive element output remains low as it begins to rise towards the ABIAS value, and the immediate post-task response is lower than the tonic value. This dependence of the post-task accommodative value on the path, or initial condition (either near or far sustained viewing), gives rise to the phenomenon of accommodative hysteresis (Fisher et al, 1987).

9.4.3 Nearwork-Induced Transient Myopia (NITM) Model

The development of myopia has both genetic and environmental components (Goss and Wickham, 1995). Although genetic factors appear to play a larger role in early-onset myopia (myopia with onset before age 15 years), modern-day work styles clearly demonstrate that environmental factors may play a significant role in the development of late-onset myopia (myopia with onset after age 15 years). A particularly important environmental factor is that of prolonged nearwork, which has been especially implicated in the development of late-onset myopia (Ong and Ciuffreda, 1995, 1997).

Quantitative measures of oculomotor parameters and dynamic responses would be helpful to differentiate between, and perhaps even predict, those who will develop myopia versus those who will not. Such a measure can be found by stimulating the accommodation system during near viewing, which

produces lenticular-based pseudo-myopia, and then measuring the closed-loop temporal course of decay of the lens response back to the original far point of accommodation. This is referred to as the nearwork-induced transient myopia (NITM) paradigm (Ehrlich, 1987; Rosenfield, *et al.*, 1992a; Ong and Ciuffreda, 1995, Jiang, 1999), with the difference between post- and pre-task values representing the NITM.

The Hung adaptation model (Hung, 1992b) discussed above quantified the effect of prolonged nearwork on the accommodative response. This model served as the basis for the simulation of NITM dynamics (Hung and Ciuffreda, 1999). An important parameter in the model, the adaptive gain, K_A, was used previously to modify the time constant of the accommodative controller, and thus controlled the rate of decay in the dark following an adaptation period. Simulations were therefore performed to determine whether variation in K_A could also account for the differences in the dynamic decay timecourse in the light following near work in the different refractive groups. In addition, the computer-simulated effect of higher K_A values on retinal defocus was examined over a 160 hr period, thus representing one work-month with 40 hours of nearwork per week, to assess its influence on the long-term development of myopia. The accommodative adaptation gain played a crucial role in inducing NITM due to its effect on the accommodative controller time constant. That is, after sustained nearwork, the increased accommodative adaptation element output would result in an increase in controller time constant. This in turn would result in a slower than normal return, or decay, of the NITM toward the pre-task baseline. Larger adaptive element gains produce slower decay rates, so that different gain values could be used to simulate NITM in the various refractive groups. It was found that the K_A values of 2.0, 2.5, 4.0 and 5.5 simulated reasonably accurately the experimental NITM time courses (Ciuffreda and Wallis, 1998) for subjects with hyperopia (HYP), emmetropia (EMM), early-onset myopia (EOM), and late-onset myopia (LOM), respectively. For simulation of the HYP group, an additional constraint was imposed wherein the accommodative response to distant stimuli was biased on the under-accommodated side of the deadspace operator. This was done for consistency with the experimental results (Ciuffreda and Wallis, 1997). In contrast, for the other three refractive groups, no such constraint was imposed so that the accommodative responses exhibited the normal slight (~ 0.25 D) over-accommodation for the far target (Rosenfield, *et al*., 1992b).

In addition, the model was used to investigate long-term effects of nearwork. There are typically alternating periods of prolonged nearwork and brief distance viewing, which is representative of our everyday activities. Under this condition, both under-accommodation at near (lag of accommodation) and over-accommodation at far (lead of accommodation) typically occur (Ciuffreda, 1991, 1998). A useful measure of the long-term

effect of the resultant retinal defocus on an individual, regardless of how it is generated, is that of the root-mean-square (rms) of the accommodative error. The rms error is essentially equal to the standard deviation about the mean value, so that a larger value is associated with greater variability in the retinal defocus. This measure was used in the prolonged nearwork simulation. This was simulated by alternating 1 hr of nearwork (3 D, 3 MA) and 5 min of far viewing (0.25 D, 0.25 MA) over a 160 hr period, which represents one work-month with 40 hours of nearwork per week. The final steady-state rms value of the overall (i.e., combined for distance and near conditions) accommodative error was measured and plotted as a function of K_A. The results show a small but progressive increase in the rms of the accommodative error with increased K_A, hence implicating this parameter in the development of myopia.

The emphasis of this model-based study was the role of the adaptive component on the NITM time course. Indeed, the NITM simulation results demonstrated that the accommodative adaptation gain K_A was clearly different for the four refractive groups. The lower adaptive gain values (K_A = 2.0 and 2.5) corresponded to the HYP and EMM groups, respectively, whereas the higher adaptive gain values (K_A = 4.0 and 5.5) corresponded to the EOM and LOM groups, respectively. The adaptive element represented a neural-oculomotor feedback process that controlled the effect of sustained stimulation of the accommodative system during nearwork. The slowed decay of the distance accommodative response following prolonged nearwork was due to an increase in output from the adaptive element, thus resulting in an increase in the accommodative controller time constant. This decay was slower for larger K_A values. The long-term increase in exposure to accommodative error, and the resultant retinal defocus, may induce increased axial length and in turn produce permanent myopia (Ong and Ciuffreda, 1997; Jiang, 1997, 1999).

9.5 SUMMARY

This chapter has provided an extensive overview of the application of bioengineering techniques to the study of the vergence system and the interactions between vergence and accommodation. In the accommodation and vergence systems, static linear and nonlinear elements serve important roles in shaping the steady-state responses and providing insight into clinical abnormalities. For example, decreased lens saturation level while maintaining normal ACG accurately simulates the AS/R curve as a function of age (Ciuffreda, 1998). Also, decreased accommodative controller gain and increased sensory-motor threshold of accommodation are associated with the visual deficits of amblyopia and congenital nystagmus, respectively.

Moreover, high AC or CA crosslink gains can lead to frank eye misalignment called strabismus, or more subtle binocular dysfunction of fusion (Hung and Ciuffreda, 1994).

Dynamic characteristics of these models have provided important insights into how these systems attain both stability and rapid motor responsivity. When each system is studied in isolation, its response characteristics provide fundamental clues regarding the system's neural control strategy. For both the accommodation and vergence systems, whose sensory latencies are long relative to their motor dynamics, a continuous feedback control process would lead to instability oscillations. It turns out that the strategy used is to respond with an initial fast open-loop movement that provides a large portion of the response amplitude, followed by a slow closed-loop movement that reduces the residual error to a minimum. In this way, both dynamic responsivity and accuracy are attained without introducing instability oscillations. However, when these systems operate together, as is generally the case in daily life, their responses are not just simple summations of their isolated motor responses, but are rather nonlinear in nature. For example, the neural linkage between the accommodation and vergence control processes results in a combined dual-interactive feedback control system that is quite complex. Additional complexity is introduced when the model is used to investigate the adaptive control of accommodation and vergence, as well as the related processes that may be involved in refractive error development. It was shown that these problems could be both conceptualized and solved using engineering feedback control systems techniques.

In the past three decades, much has been learned from these models regarding normal oculomotor control processes. Future extensions of the models include the detailed quantitative investigations of the development of myopia and ocular abnormalities such as strabismus and amblyopia, the adaptive control in the cross-links of the vergence and accommodation systems, and the interactions between visual, auditory, and perceptual cues in complex multi-media displays as well as in real-life situations. Finally, computer simulations of neurons and neural networks have the potential of improving the traditional techniques in modeling the accommodation and vergence systems.

9.6 REFERENCES

Bahill, T., and Stark, L., 1979, The trajectories of saccadic eye movements, *Sci. Am*. **240**: 108-117.

Blackie, C. A., and Howland, H., 2000, Stability analysis of two linear accommodation and convergence models, *Opt. Vis. Sci*. **77**: 608-615.

Cook, G., and Stark, L., 1967, Derivation of a model for the human eye-positioning mechanism, *Bull. Math. Biophys.* **29**: 153-175.

Ciuffreda, K. J., 1991, Accommodation and its anomalies, in: *Vision and Vision Dysfunction: Visual Optics and Instrumentation, Vol. 1,* W. N. Charman ed., Macmillan, London, pp. 231-279.

Ciuffreda, K. J., 1998, Accommodation, the pupil, and presbyopia, in: *Borish's Clinical Refraction*, W. J. Benjamin ed., W. B. Saunders Company, Philadel., PA., pp. 77-120.

Ciuffreda, K. J., and Wallis, D., 1997, Myopes show increased susceptibility to nearwork aftereffects, *Invest. Ophthal. Vis. Sci.* **39**: 1797-1803.

Eadie, A. S., Carlin, P., and Gray, L. S., 1999, Modelling vergence eye movements using fuzzy logic, in: *Current Oculomotor Research, Physiological and Psychological Aspects*, eds., W. Becker, H. Deubel, and T. Mergner, eds., Kluwer Academic/Plenum Publishers, New York, pps. 179-181.

Ebenholtz, S. M., and Fisher, S. K., 1982, Distance adaptation depends upon plasticity in the oculomotor control system, *Percept. Psychophys*. **31**: 551-560.

Ehrlich, D. L., 1987, Near vision stress: vergence adaptation and accommodative fatigue, *Ophthal. Physiol. Opt.* **7**: 353-357.

Fisher, S. K., Ciuffreda, K. J., 1988, Accommodation and apparent distance, *Perception*. **17**: 609-621.

Fisher, S. K., Ciuffreda, K. J., and Levine, S., 1987, Tonic accommodation, accommodative hysteresis, and refractive error, *Am. J. Optom. Physiol. Opt*. **64**: 799-809.

Fincham, E. F., and Walton, J., 1957, The reciprocal actions of accommodation and convergence, *J. Physiol.* **137**: 488-508.

Fry, G. A., 1939, Further experiments on the accommodation convergence relationship, *Am. J. Optom.* **16**: 325-336.

Goss, D. A., and Wickham, M. G., 1995, Retinal-image mediated growth as a mechanism for juvenile onset myopia and for emmetropization, *Doc. Ophthalmol.* **90**: 341-375.

Green, D. G., Powers, M. K., and Banks, M. S., 1980, Depth of focus, eye size and visual acuity, *Vis. Res.* **20**: 827-835.

Heath, G. G., 1956, Components of accommodation, *Am. J. Optom. Arch. Am. Acad. Optom.* **33**: 569-579.

Henson, D. B., and North, R., 1980, Adaptation to prism-induced heterophoria, *Am. J. Optom. Physiol. Opt*. **57**: 129-137.

Hofstetter, H. W., 1945, The zone of clear single binocular vision: Part 1, *Am. J. Optom. Arch. Am. Acad. Optom.* **22**: 301-333.

Hokoda, S. C., and Ciuffreda, K. J., 1983, Theoretical and clinical importance of proximal vergence and accommodation, in *Vergence Eye Movements: Basic and Clinical Aspects,* C. M Schor and K. J. Ciuffreda, eds, Butterworths, Boston, pp. 75-97.

Hung, G. K., 1998a, Dynamic model of the vergence eye movement system: simulations using MATLAB/SIMULINK, *Comp. Meth. Prog. Biomed.* **55**: 59-68.

Hung, G. K., 1998b, Sensitivity analysis of the stimulus-response function of a static nonlinear accommodation model, *IEEE. Trans. Biomed. Eng.* **45**: 335-341.

Hung, G. K., 1992a, A simple equation for relating AC/A ratio to accommodative controller gain, *Ophthal. Physiol. Opt*. **12**: 106-108.

Hung, G. K., 1992b, Adaptation model of accommodation and vergence, *Ophthal. Physiol. Opt.* **12**: 319-326.

Hung, G. K., and Ciuffreda, K. J., 1988, Dual-mode behaviour in the human accommodation system, *Ophthal. Physiol. Opt.* **8**: 327-332.

Hung, G. K., and Ciuffreda, K. J., 1994, Sensitivity analysis of relative accommodation and vergence, *IEEE. Trans. Biomed. Eng.* **41**: 241-248.

Hung, G. K., Ciuffreda, K. J., and Rosenfield, 1996, Proximal contribution to a linear static model of accommodation and vergence, *Ophthal. Physiol. Opt*. **16**: 31-41.

Hung, G. K., and Semmlow, J. L., 1980, Static behavior of accommodation and vergence: computer simulation of an interactive dual-feedback system, *IEEE. Trans. Biomed. Eng.* **27**: 439-447.

Hung, G. K., and Semmlow, J. L., 1982, A quantitative theory of control sharing between accommodative and vergence controllers, *IEEE. Trans. Biomed. Eng.* **29**: 364-370.

Hung, G. K., Semmlow, J. L., and Ciuffreda, K. J., 1986, A dual-mode dynamic model of the vergence eye movement system, *IEEE. Trans. Biomed. Eng.* **33**: 1021-1028.

Hung, G. K., Zhu, H.-M., and Ciuffreda, K. J., 1997, Convergence and divergence exhibit different response characteristics to symmetric stimuli, *Vis. Res*. **37**: 1197-1205.

Jiang, B.-C., 1996, Accommodative vergence is driven by the phasic component of the accommodative controller, *Vis. Res*. **36**: 97-102.

Jiang, B.-C., 1997, Integration of a sensory component into the accommodation model reveals differences between emmetropia and late-onset myopia, *Invest. Ophthal. Vis. Sci.* **38**: 1511-1516.

Jiang, B.-C., 1999, Oculomotor function in nearwork – induced transient and permanent myopia, *Chin. J. Optom. Ophthalmol.* **1**: 58-61 and 125-128.

Jiang, B.-C., 2000a, A modified control model for steady-state accommodation, in: *Accommodation and Vergence Mechanisms in the Visual System*, O. Franzén, H. Richter, and L. Stark, eds., Birkhäuser Verlag, Basel, Switzerland, pp. 235-243.

Jiang, B.-C., 2000b, Defocus threshold. *The VIII International Conference on Myopia, Boston, MA, 291-295.*

Jiang, B.-C., and Morse, S. E., 1999, Oculomotor functions and late-onset myopia, *Ophthal. Physiol. Opt.* **19**: 165-172.

Jiang, B.-C., and White, J. M., 1999, Effect of accommodative adaptation on static and dynamic accommodation in emmetropia and late-onset myopia, *Optom. Vis. Sci.* **76**: 295-302.

Jiang, B.-C., and Woessner, W. M., 1996, Dark focus and dark vergence: an experimental verification of the configuration of the dual-interactive feedback model, *Ophthal. Physiol. Opt.* **16**: 342-347.

Jones, R. 1980, Fusional vergence: sustained and transient components, *Am. J. Optom. Physiol. Opt.* **57**: 640-644.

Jones, R., and Kerr, K., 1971, Motor responses to conflicting asymmetrical vergence stimulus information, *Am. J. Optom*. **48**: 989-1000.

Jones, R., and Kerr, K., 1972, Vergence eye movements to pairs of disparity stimuli with shape selection cues, *Vis. Res*. **12**: 1425-1430.

Kotulak, J. C., and Schor, C. M., 1986a, The accommodative response to subthreshold blur and to perceptual fading during the Troxler phenomenon, *Perception.* **15**: 7-15.

Kotulak, J. C., and Schor, C. M., 1986b, Temporal variations in accommodation during steady-state conditions, *J. Opt. Soc. Am. A.* **3**: 223-227.

Krishnan , V. V. , and Stark , L., 1975, Integral control in accommodation, *Comp. Prog. Biomed*. **4**: 237-255.

Krishnan, V. V., and Stark, L., 1977, A heuristic model for the human vergence eye movement system, *IEEE. Trans. Biomed. Eng.* **24**: 44-49.

Ludvigh, E., McKinnon, P., and Zartzeff, L., 1964, Temporal course of the relaxation of binocular duction (fusion) movements, *Arch. Ophthalmol.* **71**: 389-399.

Maddox, E. E., 1893, *The Clinical Use of Prisms; and the Decentering of Lenses*. 2nd ed. Bristol, England: John Wright & Sons.

Mordi, J. A., 1991, *Accommodation, Age and Presbyopia*, Ph.D. Dissertation. State Univ. of New York, State College of Optometry, New York, U.S.A.

Mordi, J. A., and Ciuffreda, K. J., 1998, Static aspects of accommodation: age and presbyopia, *Vis. Res.* **38**: 1643-1653.

Morgan, M. W., 1983, The Maddox analysis of vergence, in: *Vergence Eye Movements: Basic and Clinical Aspects*, C.M. Schor and K. J. Ciuffreda eds., Butterworths, Boston, pp. 15-21.

North, R. V., Henson, D. B., and Smith, T. J., 1993, Influence of proximal, accommodative and disparity stimuli upon the vergence system, *Ophthal. Physiol. Opt*. **13**: 239-243.

Ogle, K. N., 1972, *Researches in Binocular Vision*. Hafner, New York, pp. 59-93.

Ogle, K. N., Martens, T. G., and Dyer, J. A., 1967, *Binocular Vision and Fixation Disparity.* Lea and Febiger, Philadel., PA, pp. 9-119.

Ong, E., and Ciuffreda, K. J., 1995, Nearwork-induced transient myopia – a critical review, *Doc Ophthalmol.* **91**: 57-85.

Ong, E., and Ciuffreda, K. J., 1997, *Accommodation, Nearwork, and Myopia,* Optometric Extension Program Foundation, Inc., Santa Ana, CA.

O'Shea, W. F., Ciuffreda, K. J., Fisher, S. K., Tannen, B., and Super, P., 1988, Relation between distance heterophoria and tonic vergence, *Am. J. Optom. Physiol. Opt.* **65**: 787-793.

Owens, D. A., 1984, The resting state of the eyes, *Am. Sci.* **72**: 378-387.

Owens, D. A., and Leibowitz, H. W., 1980, Accommodation, convergence, and distance perception in low illumination, *Am. J. Optom. Physiol. Opt.* **57**: 540-550.

Owens, D. A., and Tyrrell, R. A., 1992, Lateral phoria at distance: contribution of accommodation, *Invest. Ophthal. Vis. Sci.* **33**: 2733-2743.

Patel, S. S., 1995, A neural network model of short-term dynamics of human disparity vergence system, Ph.D. Dissertation, Univ. of Houston, Houston, TX.

Patel, S. S., Ogmen, H., White, J. M., and Jiang, B., 1997, Neural network model of short-term horizontal disparity vergence dynamics, *Vis. Res.* **37**: 1383-1399.

Pobuda, M., and Erkelens, C. J., 1993, The relationship between absolute disparity and ocular vergence, *Biol. Cyber.* **68**: 221-228.

Rashbass, C., and Westheimer, G., 1961, Disjunctive eye movements, *J. Physiol.* **159**: 339-360.

Ripps, H., Chin, N. B., Siegel, I. M., and Breinin, G. M., 1962, The effect of pupil size on accommodation, convergence, and the AC/A ratio, *Invest. Ophthal. Vis. Sci.* **1**: 127-135.

Rosenfield, M., Ciuffreda, K. J., and Chan, H.-W., 1995, Effects of age on the interaction between AC/A and CA/C ratios, *Ophthal. Physiol. Opt*. **15**: 451-455.

Rosenfield, M., Ciuffreda, K. J., and Hung, G. K., 1991, The linearity of proximally induced accommodation and vergence, *Invest. Ophthal. Vis. Sci*. **32**: 2985-2991.

Rosenfield, M., Ciuffreda, K. J., and Novogrodsky, L., 1992a, Contribution of accommodation and disparity-vergence to transient nearwork-induced myopic shifts, *Ophthal. Physiol. Opt.* **12**: 433-436.

Rosenfield, M., Ciuffreda, K. J., and Rosen, J., 1992b, Accommodative response during distance optometric test procedures. *J. Am. Optom. Assoc.* **63**: 614-618.

Rosenfield, M., and Gilmartin, B., 1990, Effect of target proximity on the open-loop accommodative response, *Optom. Vis. Sci*. **67**: 74-79.

Schor, C. M., 1979, The relationship between fusional vergence and fixation disparity, *Vis. Res.* **19**: 1359-1367.

Schor, C. M., 1985, Models of mutual interactions between accommodation and convergence, *Am. J. Optom. Physiol. Opt.* **62**: 369-374.

Schor, C. M., 1992, A dynamic model of cross-coupling between accommodation and convergence: simulation of step and frequency responses. *Optom. Vis. Sci.* **69**: 258-269.

Schor, C. M., 1999, The influence of interactions between accommodation and convergence on the lag of accommodation, *Ophthal. Physiol. Opt.* **19**: 134-150.

Schor, C. M., and Horner, D., 1989, Adaptive disorders of accommodation and vergence in binocular dysfunction, *Ophthal. Physiol. Opt.* **9**: 264-268.

Schor, C. M., and Kotulak, J. C., 1986, Dynamic interactions between accommodation and convergence are velocity sensitive, *Vis. Res*. **26**: 927-942.

Semmlow, J. L., and Hung, G. K., 1983, The near response: theories of control, in: *Vergence Eye Movements: Basic and Clinical Aspects*, C.M. Schor and K. J. Ciuffreda eds., Butterworths, Boston, pp. 175-195.

Semmlow, J. L., Hung, G. K., and Ciuffreda, K. J., 1986, Quantitative assessment of disparity vergence components, *Invest. Ophthal. Vis. Sci.* **27**: 558-564.

Semmlow, J. L., Hung, G. K., Horng, J.-L., and Ciuffreda, K. J., 1993, Initial control component in disparity vergence eye movements, *Ophthal. Physiol. Opt*. **13**: 48-55.

Sethi, B., and North, R. V., 1987, Vergence adaptive changes with varying magnitudes of prism-induced disparities and fusional amplitudes, *Am. J. Optom. Physiol. Opt*. **64**: 263-268.

Stark, L., Kenyon, R. V., Krishnan, V. V., and Ciuffreda, K. J., 1980, Disparity vergence: A proposed name for a dominant component of binocular vergence eye movements, *Am. J. Optom. Physiol. Opt*. **57**: 606-609.

Toates, F. M., 1972, Further studies on the control of accommodation and convergence, *Measurement and Control.* **5**: 58-61.

Toates, F. M. 1974, Vergence eye movements, *Doc. Ophthal*. **37**: 153-214.

Toates, F. M., 1975, *Control Theory in Biology and Experimental Physiology,* Hutchinson, London.

Westheimer, G., 1963, Amphetamine, barbiturates and accommodation-convergence, *Arch. Ophthal*. **70**: 830-836.

Westheimer, G., Mitchell, A. M., 1956, Eye movement responses to convergence stimuli, *Arch. Ophthalmol*. **55**: 848-856.

Wick, , B., 1985, Clinical factors in proximal vergence, *Am. J. Optom. Physiol. Opt*. **62**: 1-18.

Windhorst, U., 1996, Spinal cord and brainstem: Pattern generators and reflexes, in Greger R and U. Windhorst, eds., *Comprehensive Human Physiology: From Cellular Mechanisms to Integration, Vol. 1*, Springer-Verlag, Berlin, pp. 1007-1032.

Wolf, K. S., Bedell, H. E., and Pedersen, S. B., 1990, Relations between accommodation and vergence in darkness, *Optom. Vis. Sci.* **67**: 89-93.

Wong, L., and Jiang, B.-C., 2000, Stimulus/response threshold of accommodation in emmetropes and myopes, *Invest. Ophthal. Vis. Sci*. **41**: S816.

Zadeh, L., 1965, Fuzzy sets, *Inf. Control*. **8:** 338-353.

Zadeh, L., 1994, The Role of Fuzzy Logic in Modeling, Identification and Control, *Modeling Identification and Control*. **15**: 191-203.

Zuber, B., and Stark, L., 1968, Dynamical characteristics of fusional vergence eye movement system, *IEEE Trans. Sys. Sci. Cybern*. **4**: 72-79.